Simulation and Analysis of Physical Processes for Aiding Technology Development

Dan Cole

Dept. Manufacturing Engineering, Boston University

Simulation of Physical Processes

- Approaches range from very fundamental to fairly phenomenological/empirical directions
- The stage of technology helps to dictate the appropriate level of simulation/modeling.
- Both directions are useful! One is more predictive, but more computationally intensive; the other is less predictive, more reliant on measurements, but much faster.

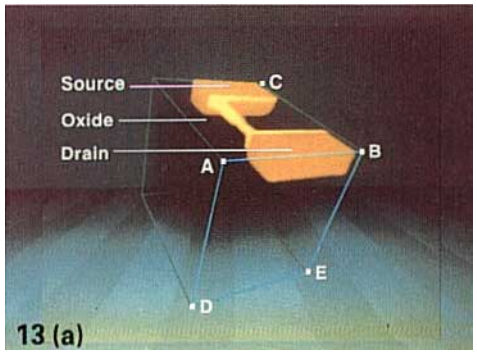

Examples of Simulation Aiding Technology Development

Micro/nano lithography

SPIE 2003 (two articles)
Applied Phys. Lett. 2002
SPIE 2002
Proc. IEEE 2001
SPIE 1999 (two articles)
Funding from SEMATECH

Metrology

SPIE 2003, 1999
Applied Phys. Lett. 2002
IEEE Trans. Semi. Manufacturing (submitted)

Rydberg Atom Analysis

J. Scientific Computation 2003 (two)
J. Computational Phys. (two submitted)
Funding from CIPA

Casimir Forces

Foundations of Physics 2000
Foundations of Physics 1999
Presentations at several conferences, including NASA and international workshop at Harvard
Funding from CIPA

Compact Modeling

Articles in progress
Presentations at industry conferences
Funding from IBM

Rydberg Atom Simulation

- Involves behavior of electron in highly excited state, or, electron in hydrogen atom.

- Reasons for studying:

  - Effect behavior of outer electron
  - Possibly be able to “store” and “read” information on state of outer electron
  - Control ionization - ion implantation and plasma etching
  - Beginnings of being able to control/modify chemical reactions electromagnetically.
  - Scientifically, excellent system to investigate regarding chaos in classical system versus quantum chaos. Scarring.

Classical

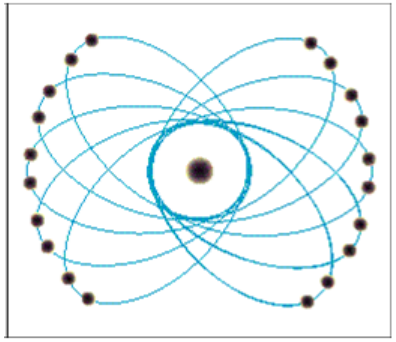

Quantum

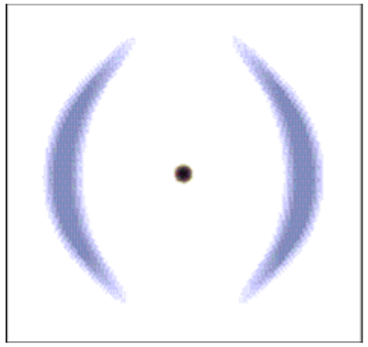

Rydberg Atom Simulation

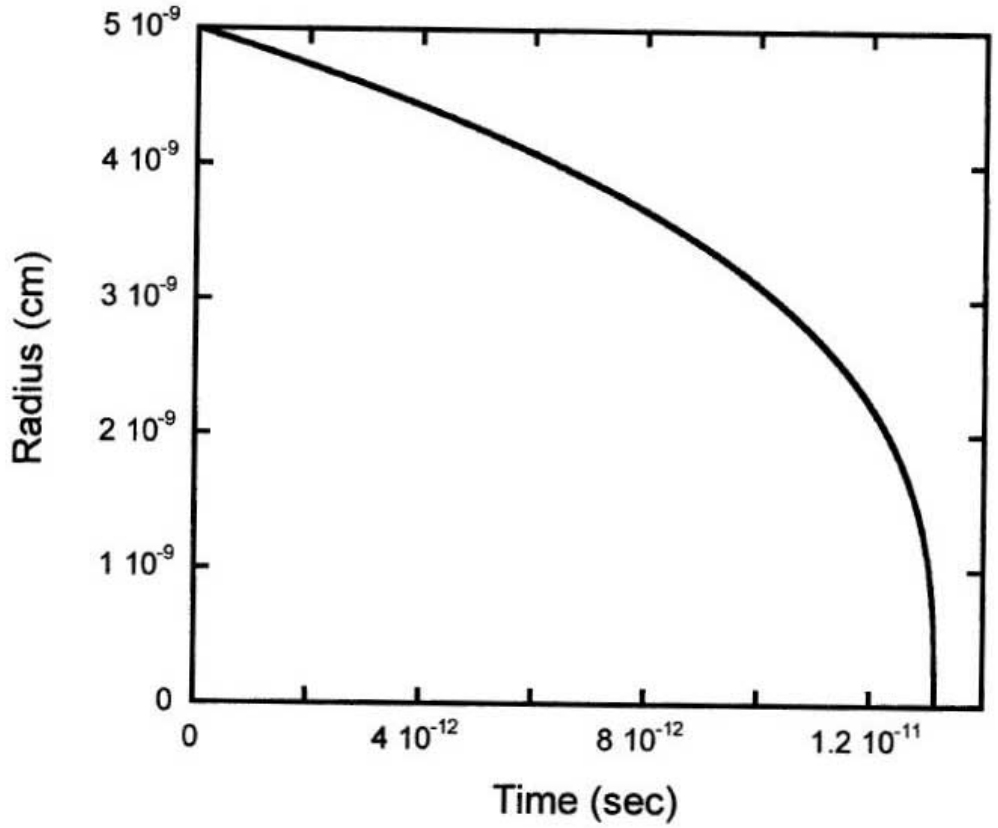

Classical

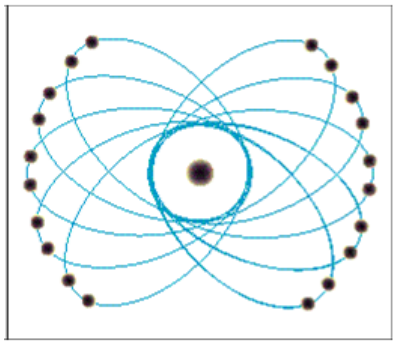

Quantum

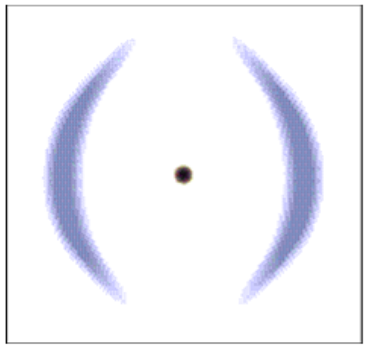

Rydberg Atom Simulation

Equation of motion is the Lorentz-Dirac equation.
In relativistic notation:

$$m\frac{d^2z^\mu}{d\tau^2} = \frac{2e^2}{3c^3}\left[\frac{d^3z^\mu}{d\tau^3} - \frac{1}{c^2}\left(\frac{d^2z^\lambda}{d\tau^2}\frac{d^2z_\lambda}{d\tau^2}\right)\frac{dz^\mu}{d\tau}\right] + F^\mu$$

In 3-vector notation this equation is, with $\gamma \equiv \left[1-(\dot{\mathbf{z}}/c)^2\right]^{-1/2}$:

$$\frac{d}{dt}(\gamma m\dot{\mathbf{z}}) = -\frac{e^2\mathbf{z}}{|\mathbf{z}|^3} + \mathbf{R}_{\text{reac}} + (-e)\left\{\mathbf{E}[\mathbf{z}(t),t] + \frac{\dot{\mathbf{z}}}{c}\times\mathbf{B}[\mathbf{z}(t),t]\right\}$$

where the radiation reaction is:

$$\mathbf{R}_{\text{reac}} = \frac{2e^2}{3c^3}\left\{\frac{d}{dt}\left[\gamma^2\ddot{\mathbf{z}} + \gamma^4\left(\frac{\dot{\mathbf{z}}}{c}\cdot\ddot{\mathbf{z}}\right)\frac{\dot{\mathbf{z}}}{c}\right] - \frac{1}{c}\left[\gamma^4\ddot{\mathbf{z}}^2 + \gamma^6\left(\frac{\dot{\mathbf{z}}}{c}\cdot\ddot{\mathbf{z}}\right)^2\right]\frac{\dot{\mathbf{z}}}{c}\right\}.$$

Rydberg Atom Simulation

The nonrelativistic approximation to the Lorentz-Dirac equation is:

$$m\ddot{\mathbf{z}} = -\frac{e^2\mathbf{z}}{|\mathbf{z}|^3} + \mathbf{R}_{\text{reac}} + (-e)\left\{\mathbf{E}[\mathbf{z}(t),t] + \frac{\dot{\mathbf{z}}}{c} \times \mathbf{B}[\mathbf{z}(t),t]\right\}$$

where:

$$\mathbf{R}_{\text{reac}} \approx \frac{2}{3}\frac{e^2}{c^3}\frac{d^3\mathbf{z}}{dt^3} \approx \frac{2}{3}\frac{e^2}{c^3}\frac{d}{dt}\left[-\frac{e^2\mathbf{z}}{m|\mathbf{z}|^3}\right]$$

Rydberg Atom Simulation

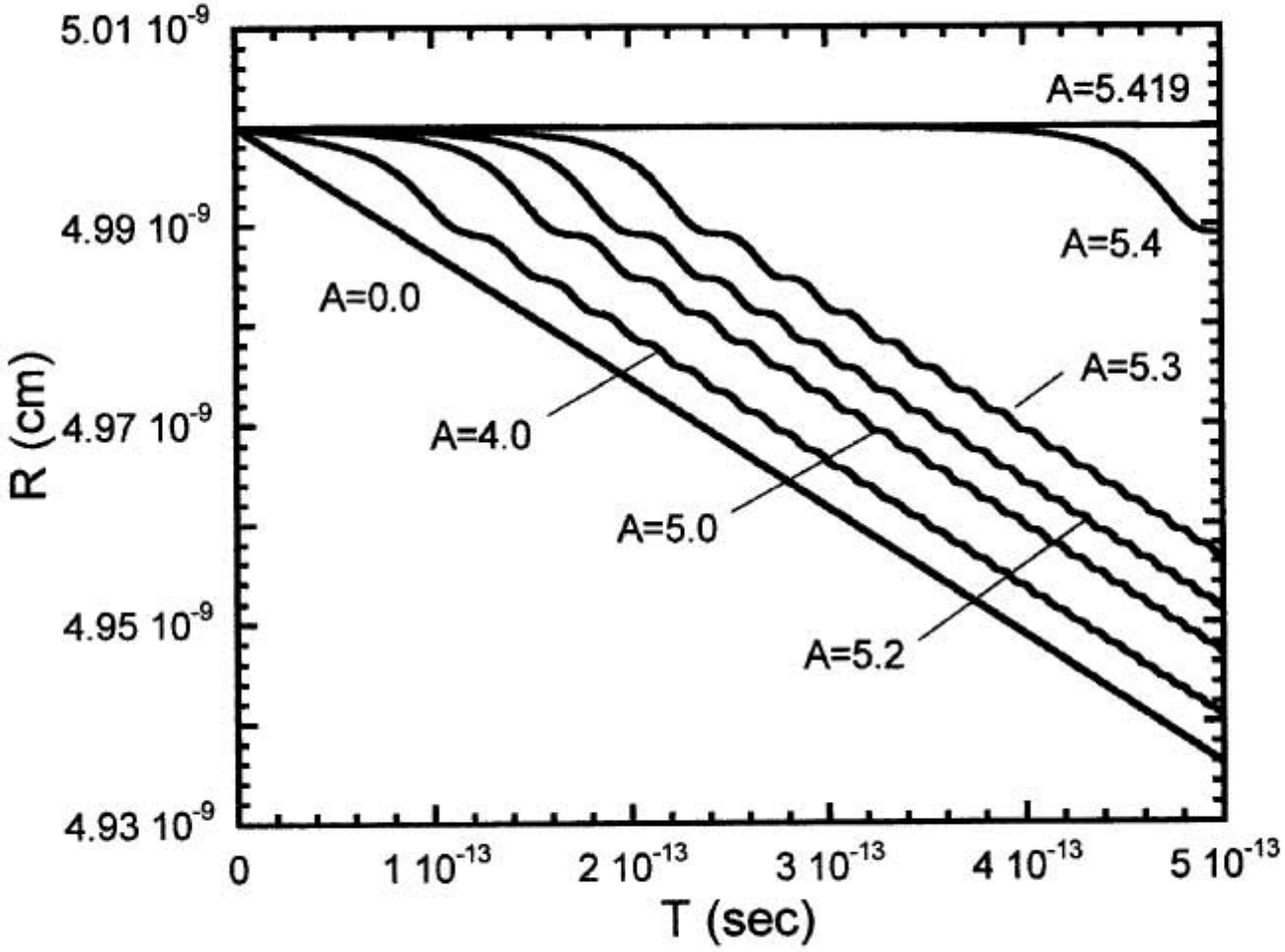

Rydberg Atom Simulation

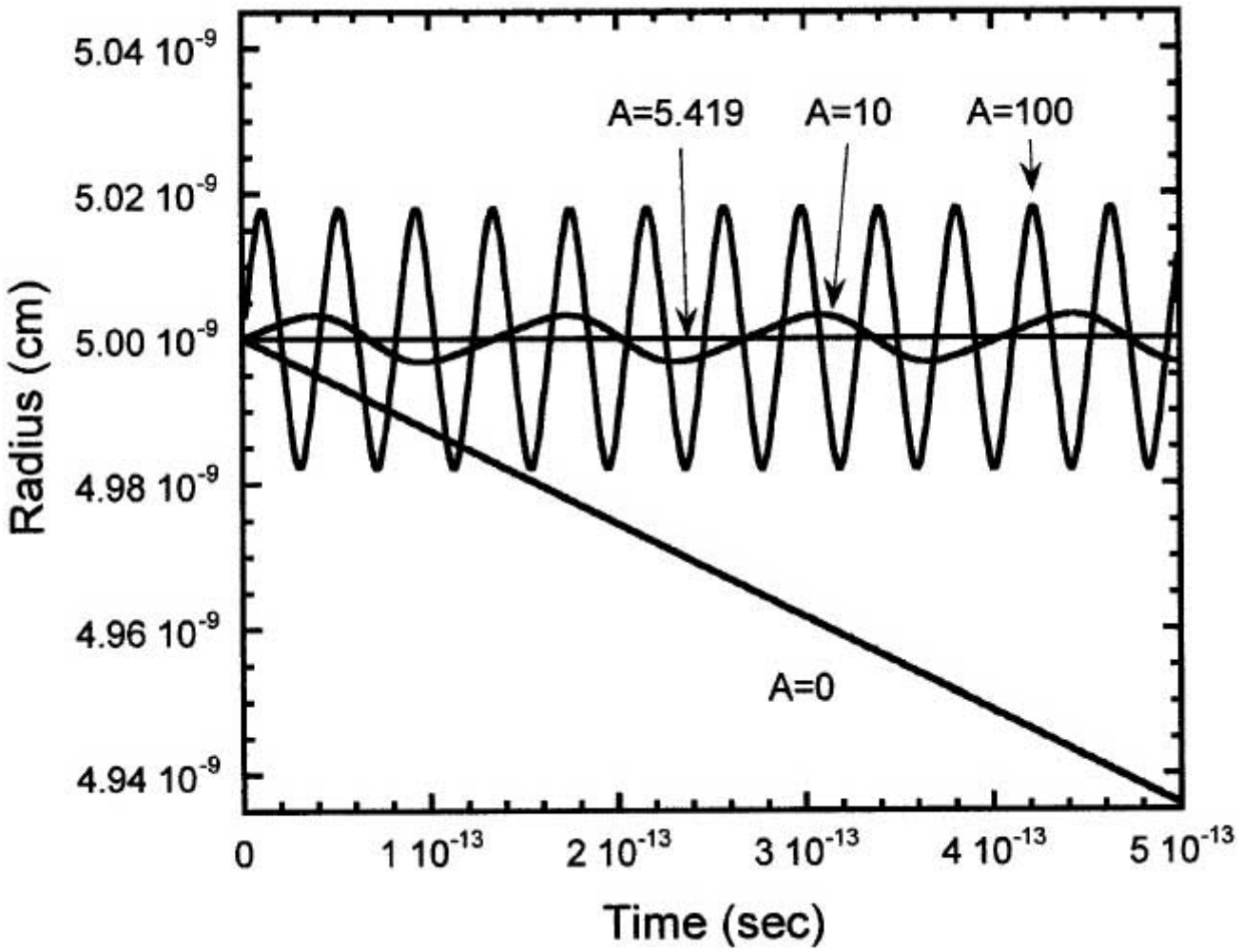

Rydberg Atom Simulation

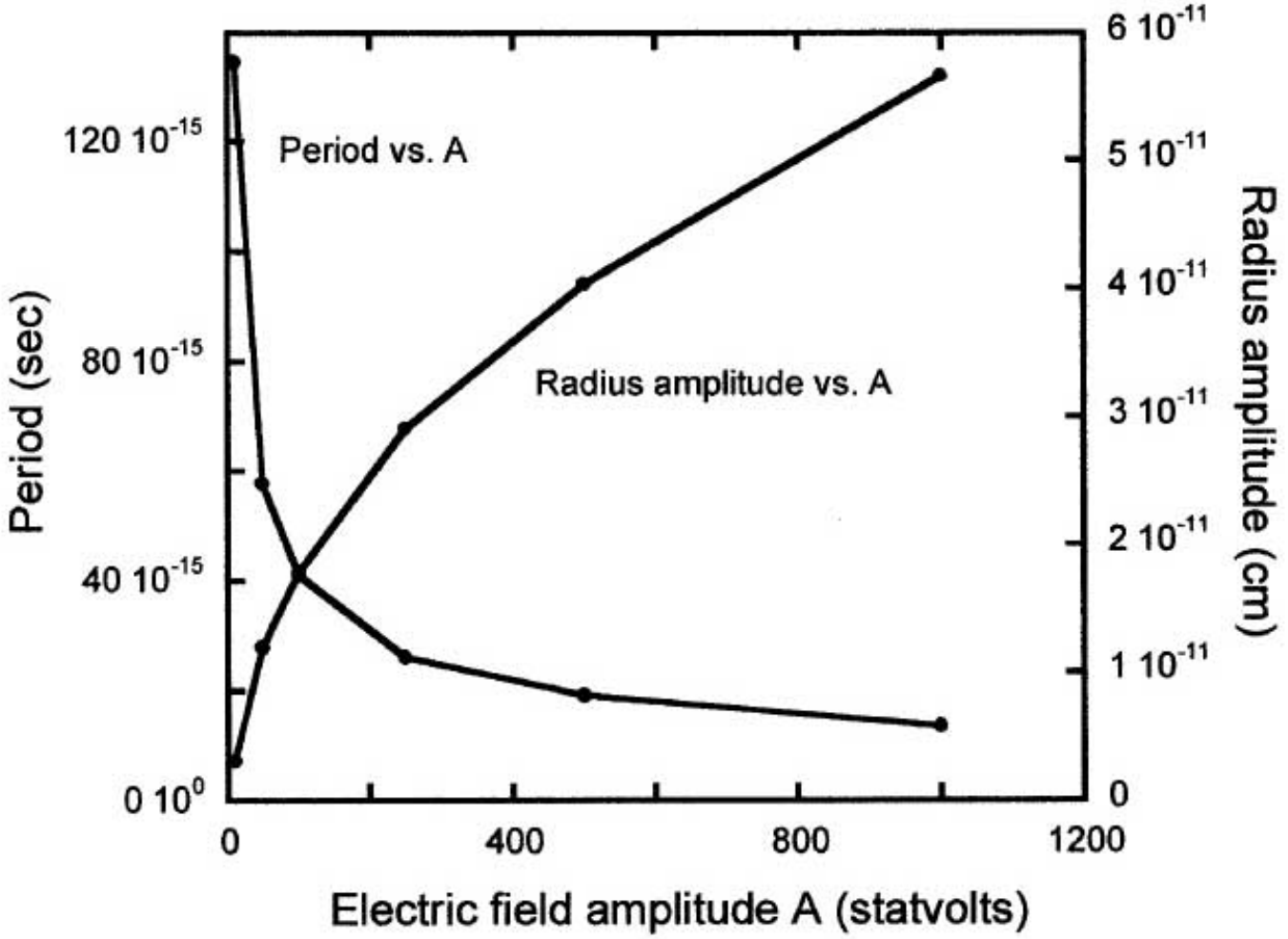

Rydberg Atom Simulation

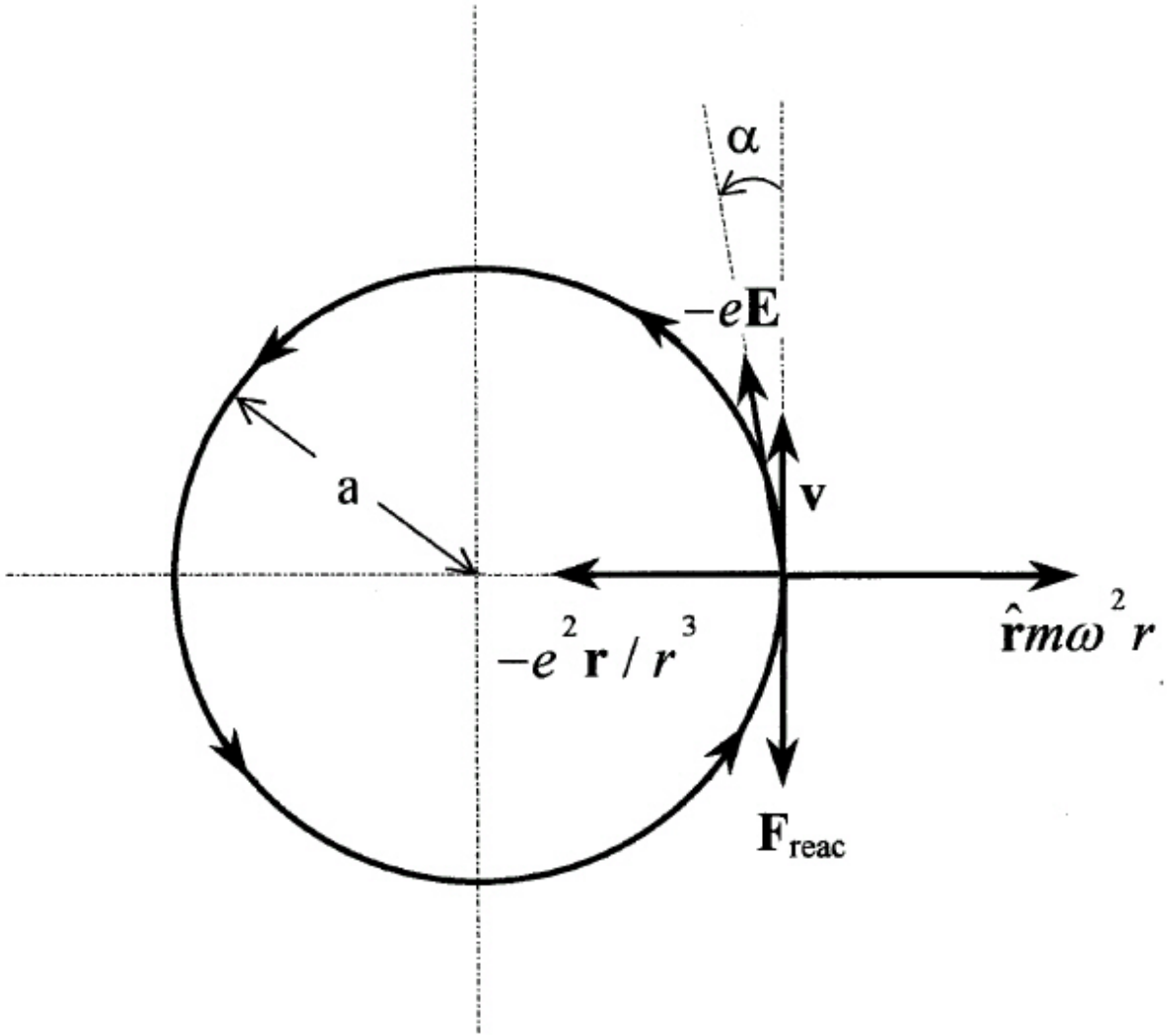

Rydberg Atom Simulation

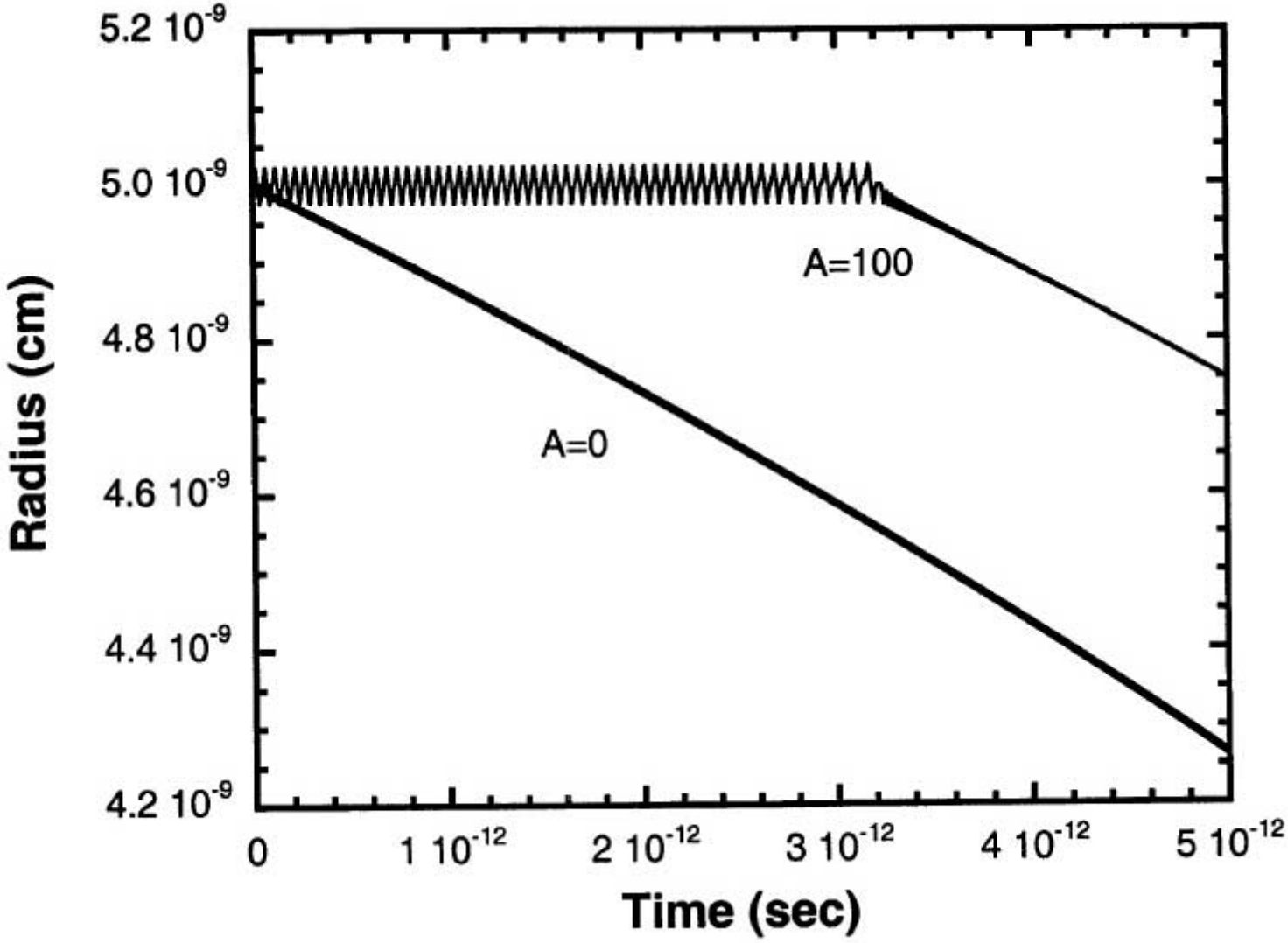

Rydberg Atom Simulation

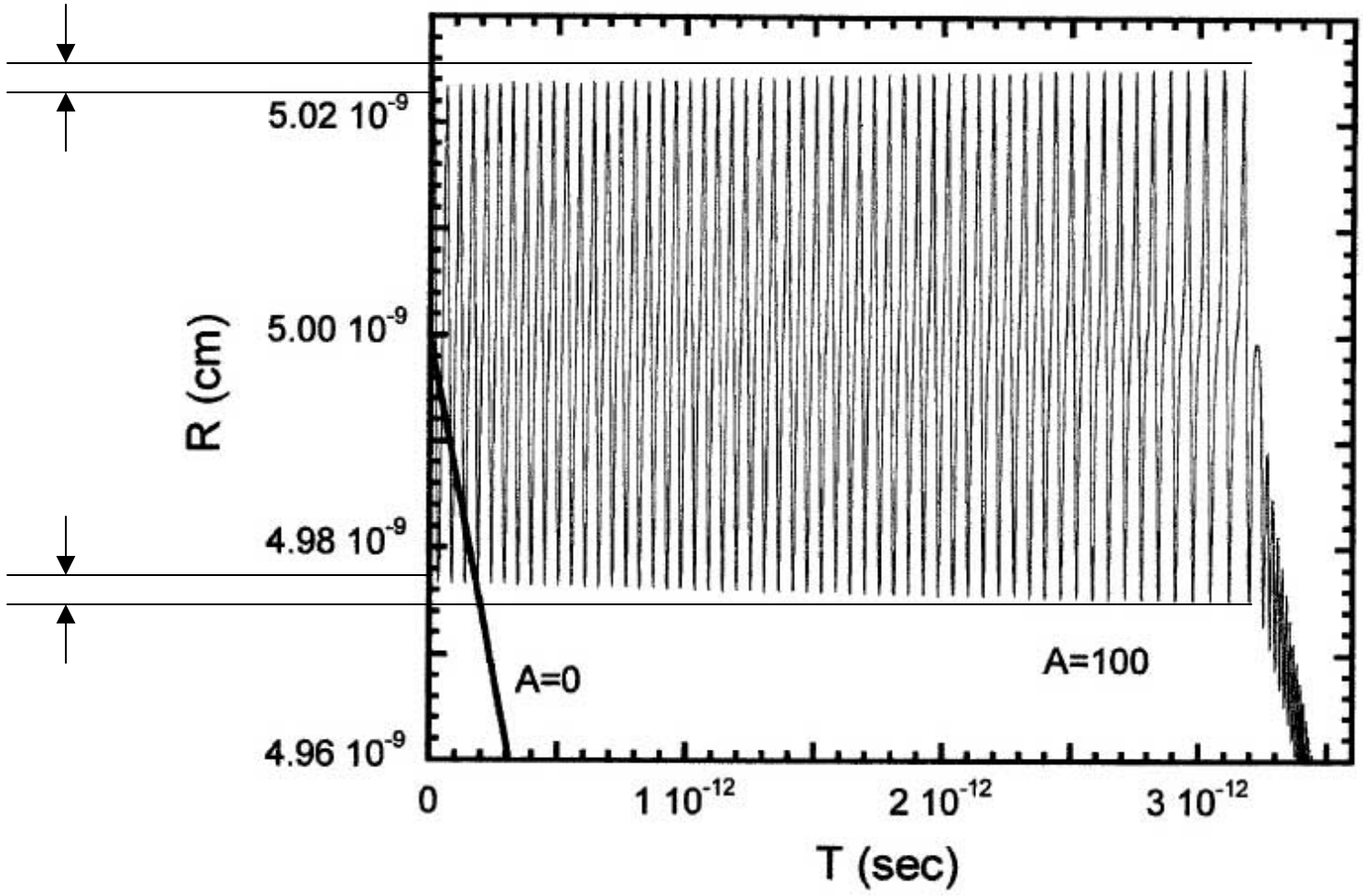

Rydberg Atom Simulation

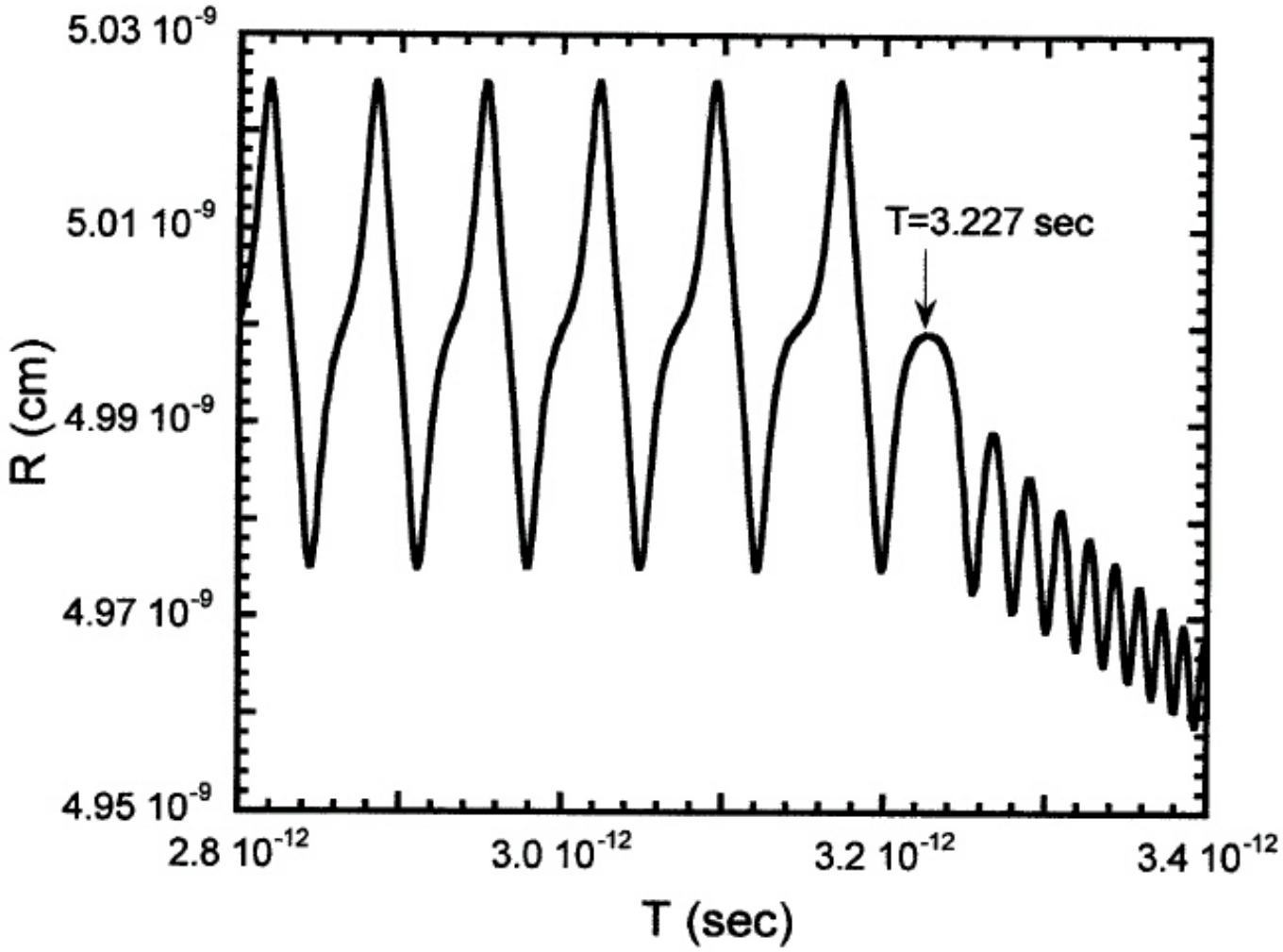

Rydberg Atom Simulation

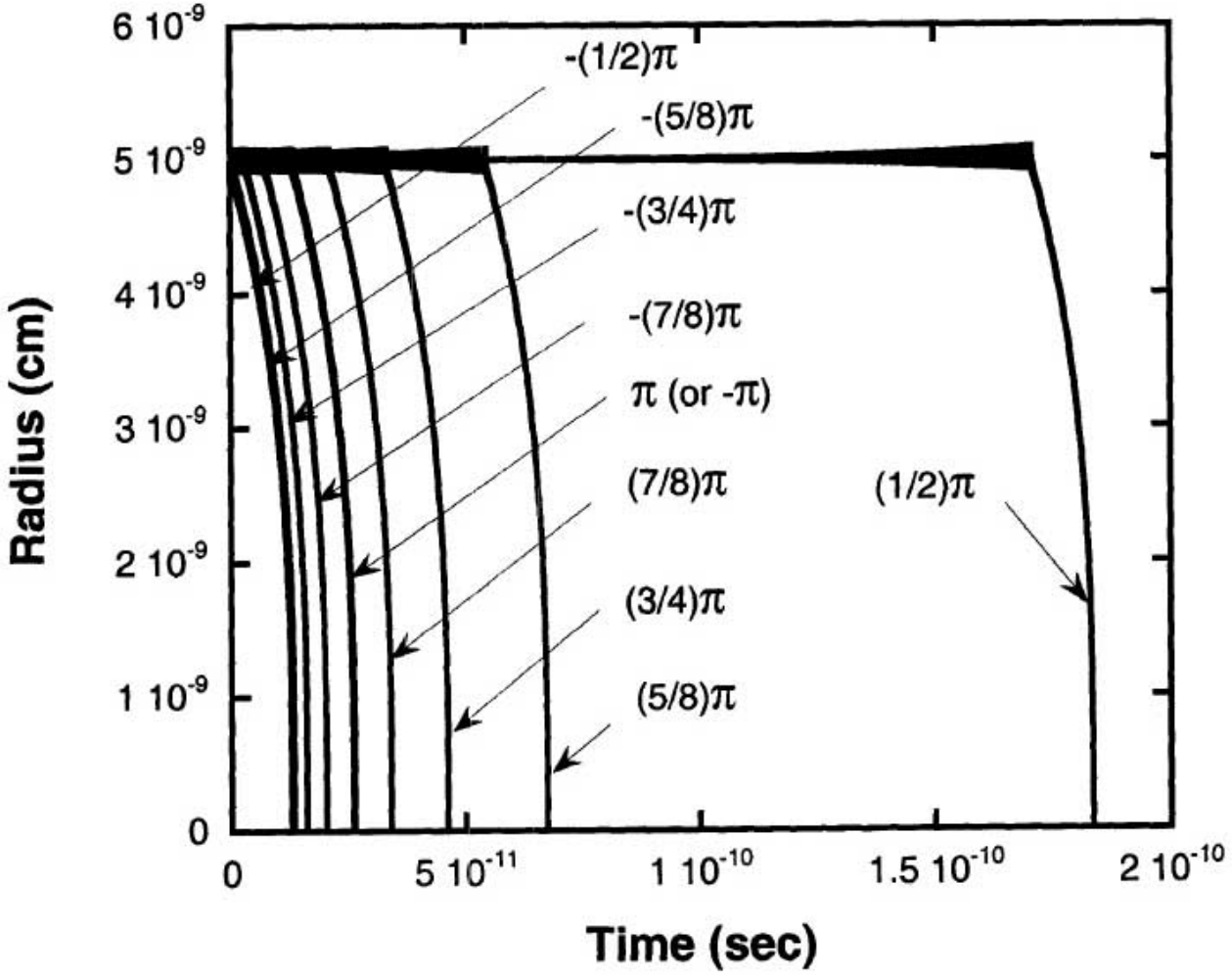

Rydberg Atom Simulation

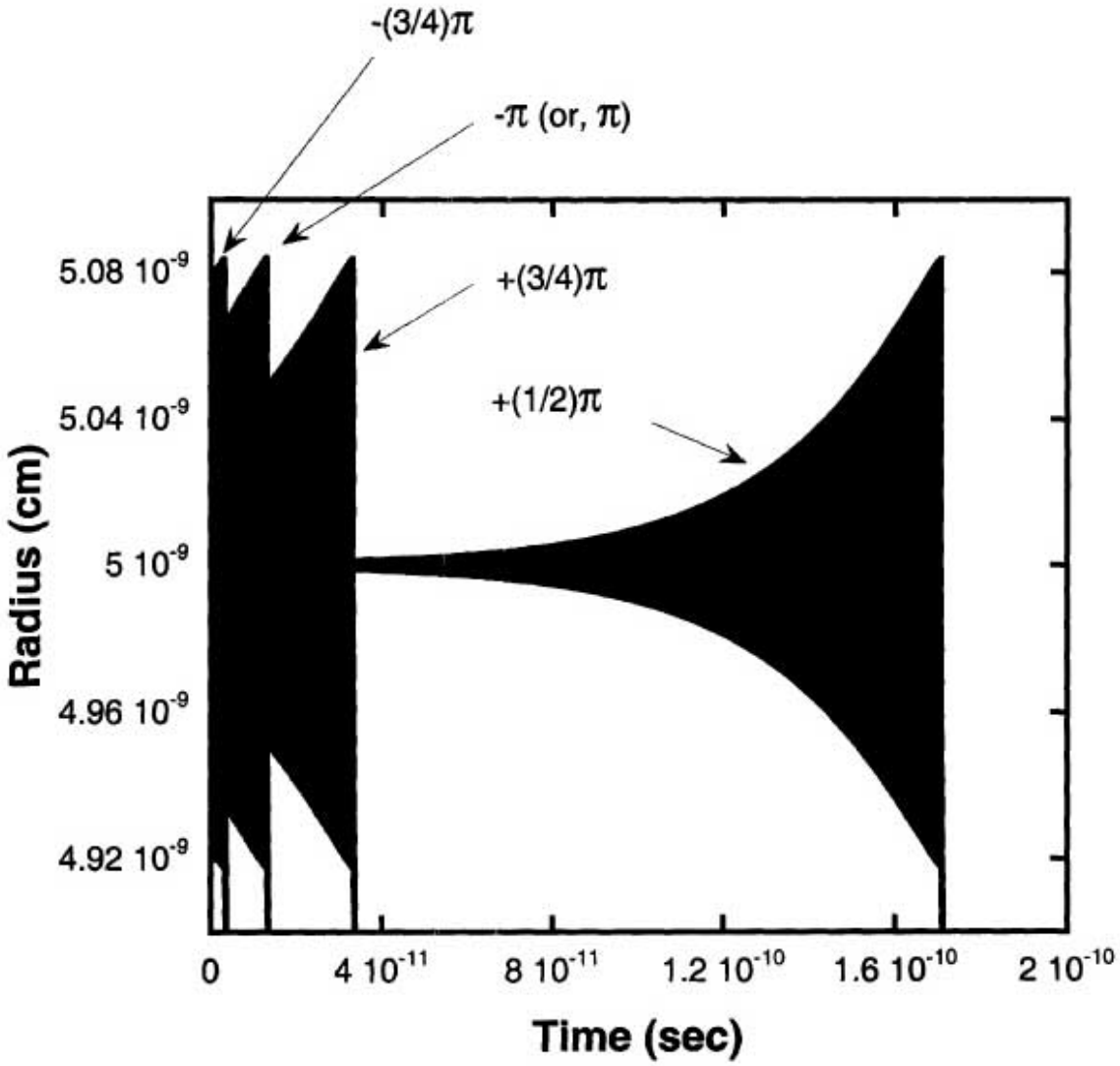

Rydberg Atom Simulation

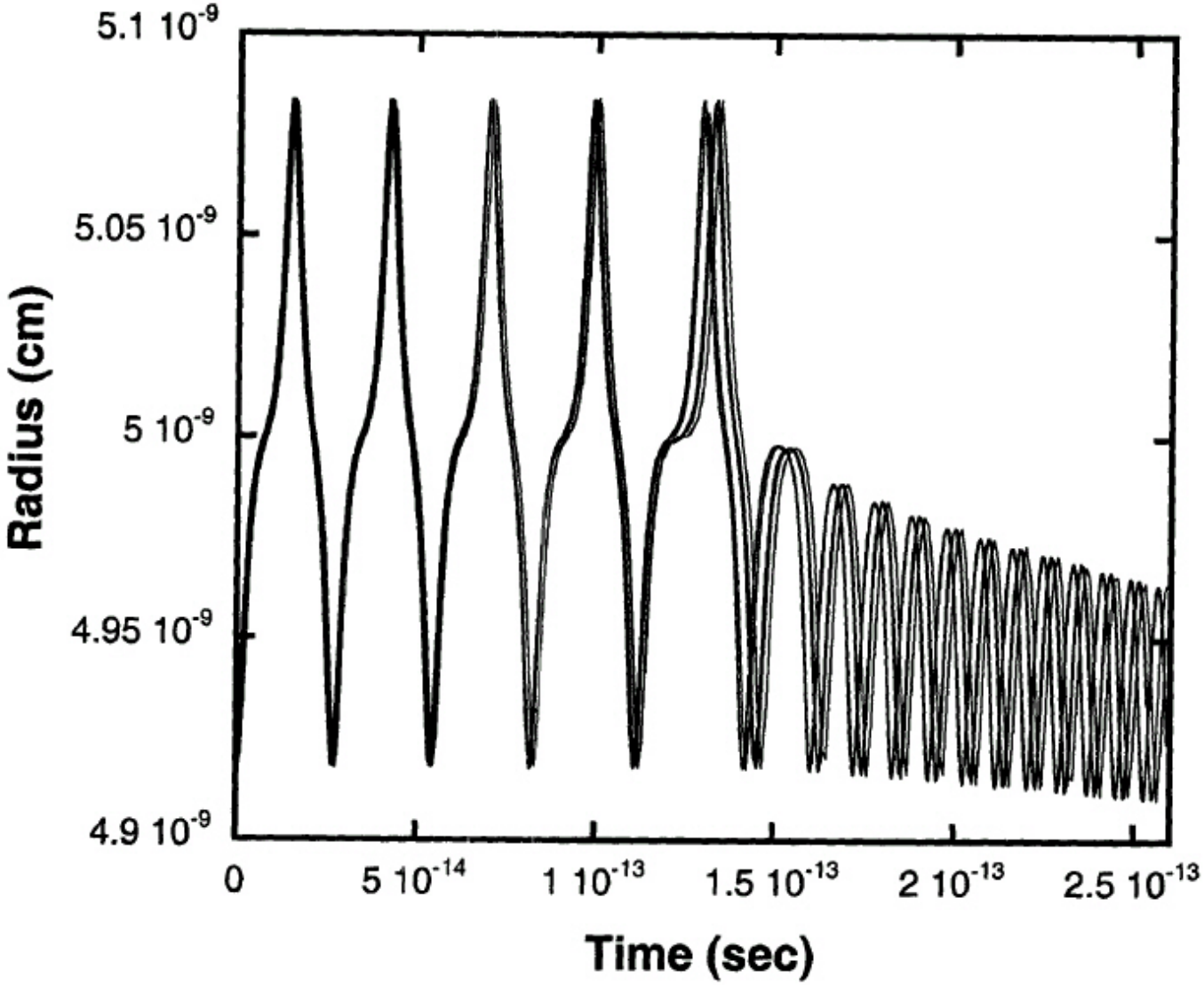

Rydberg Atom Simulation

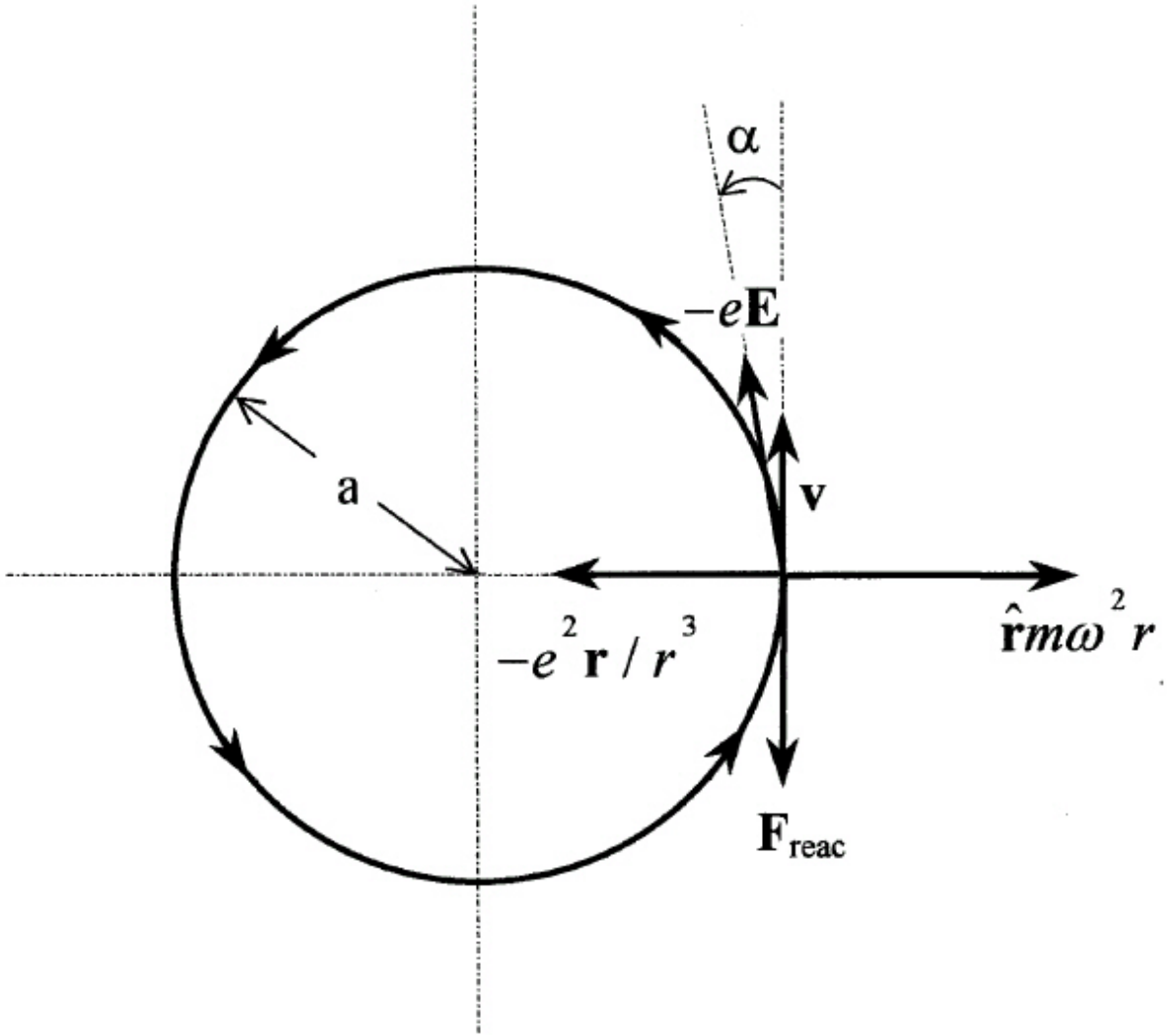

Rydberg Atom Simulation

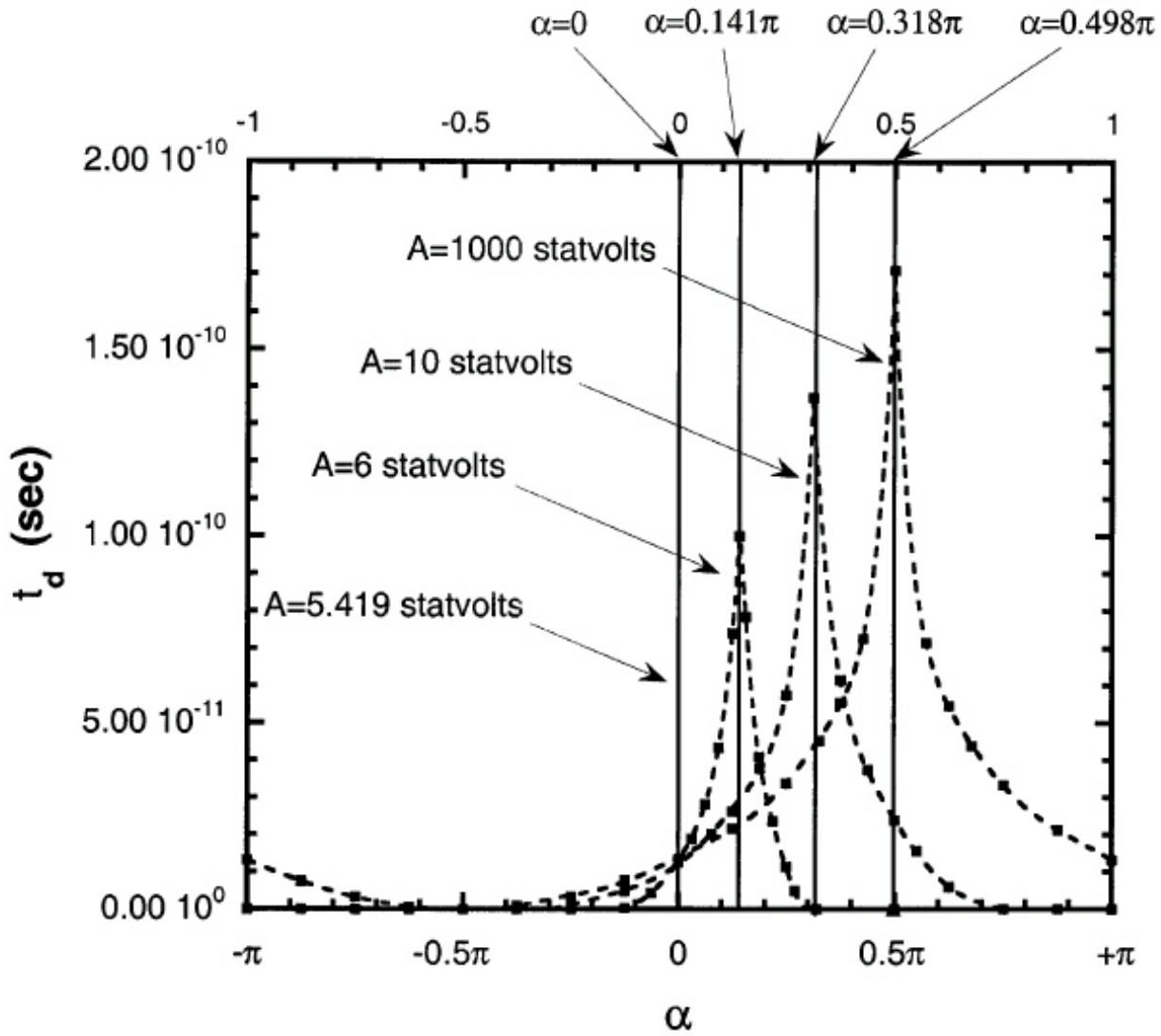

Rydberg Atom Simulation

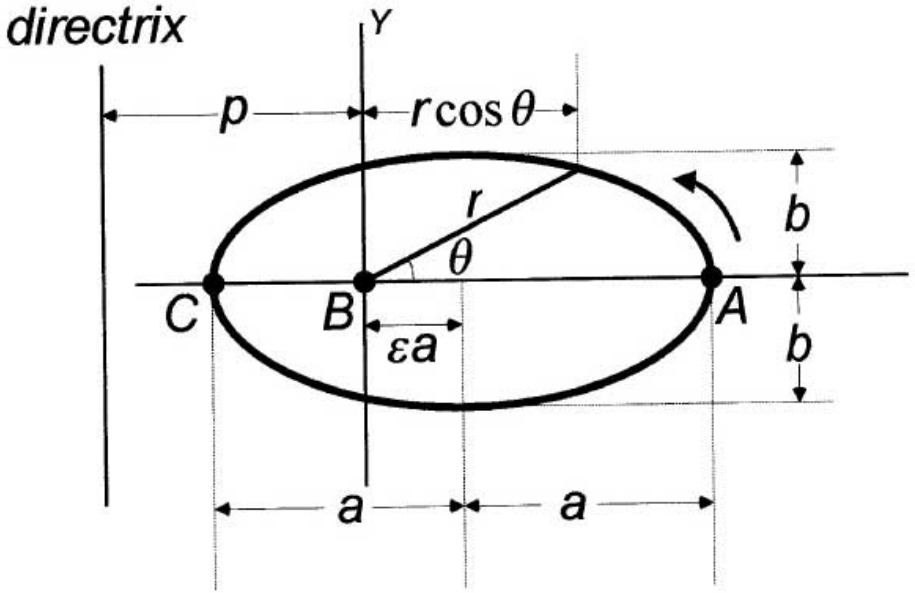

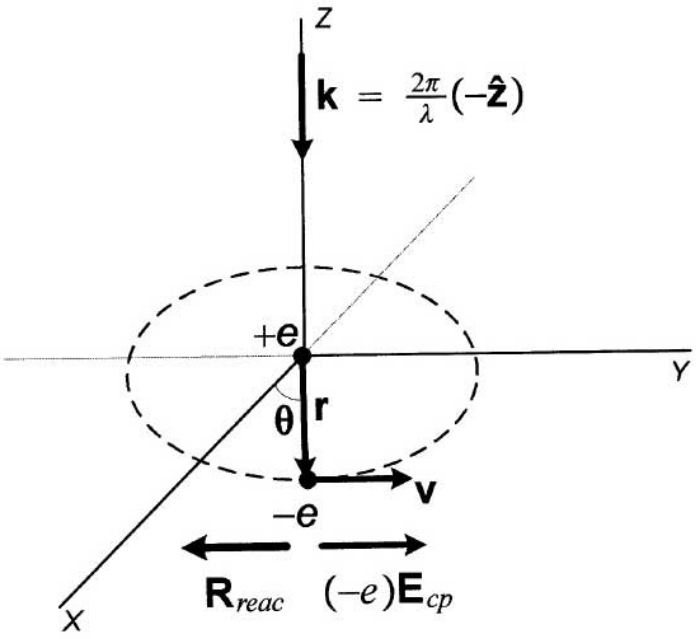

Rydberg Atom Simulation

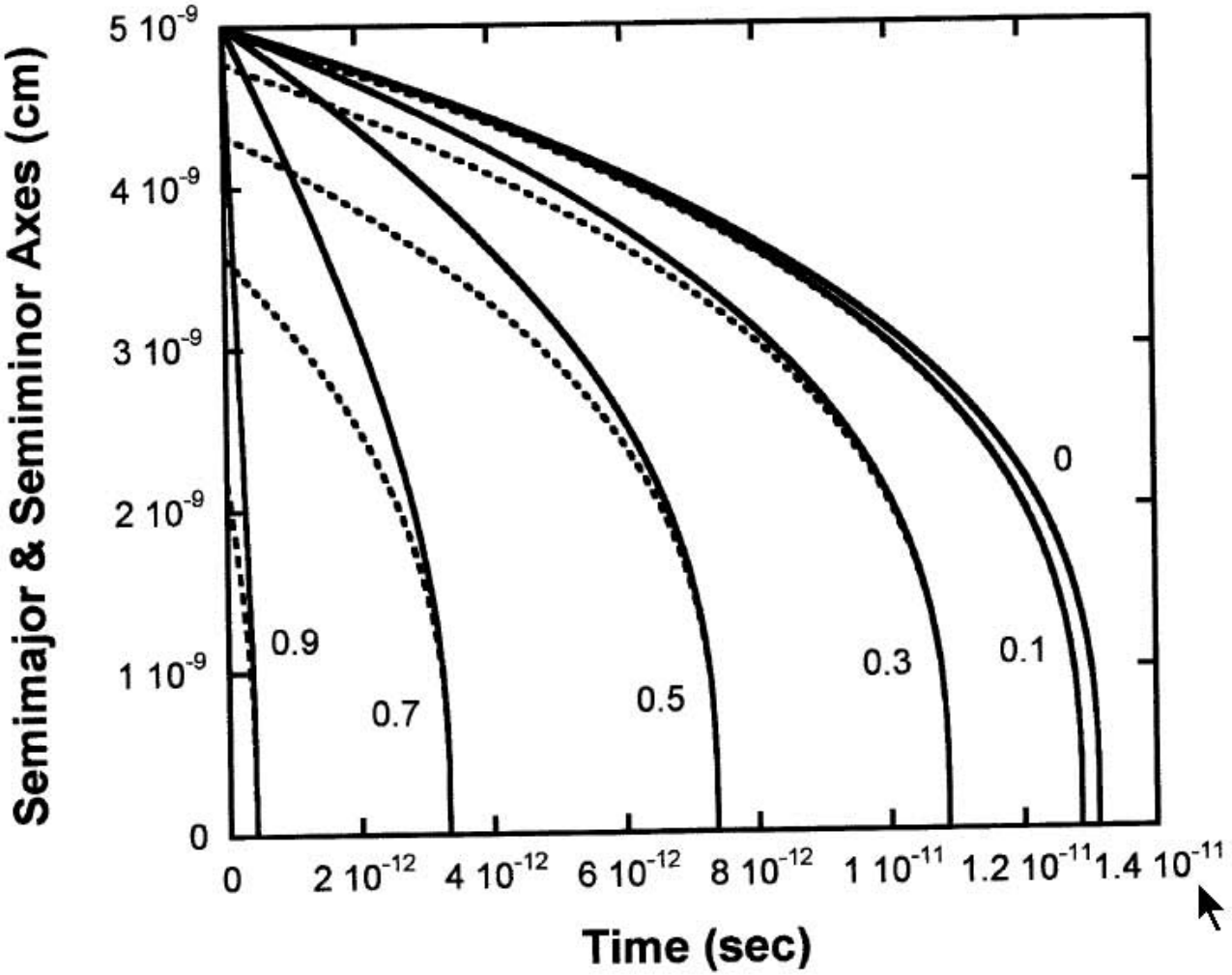

Casimir Force Analysis and Simulation

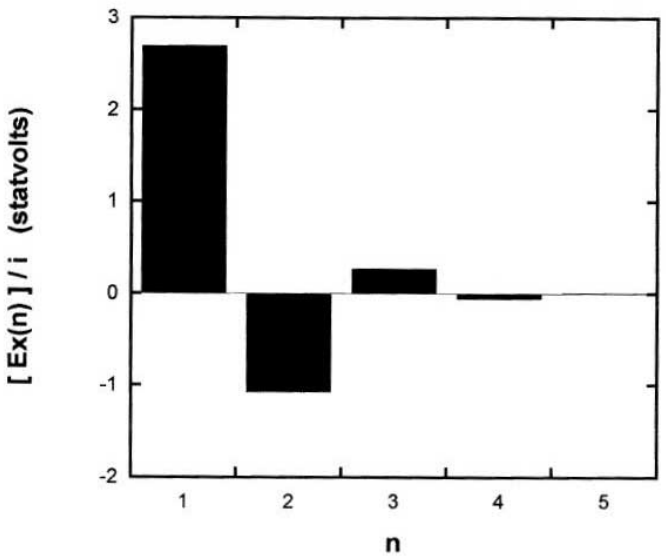

$\varepsilon = 0.1$

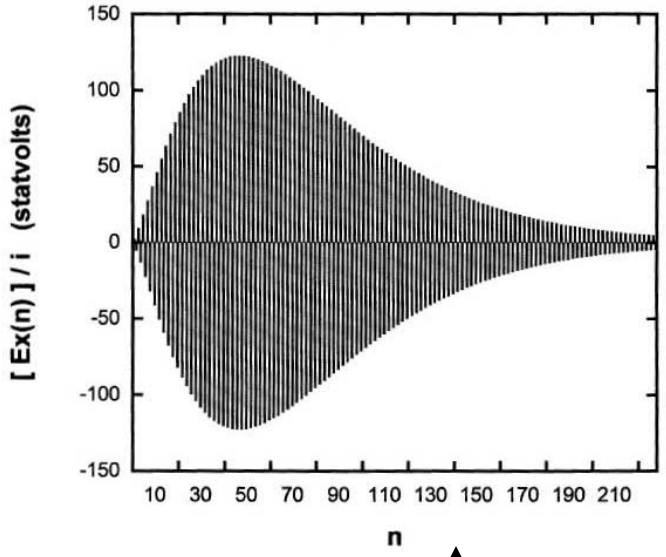

$\varepsilon = 0.9$

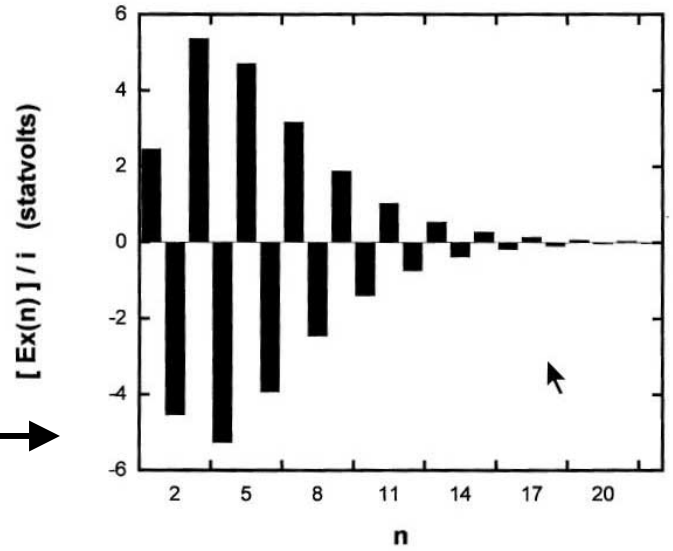

$\varepsilon = 0.5$

$$\varepsilon = \sqrt{1 - \left(\frac{b}{a}\right)^2}$$

Rydberg Atom Simulation

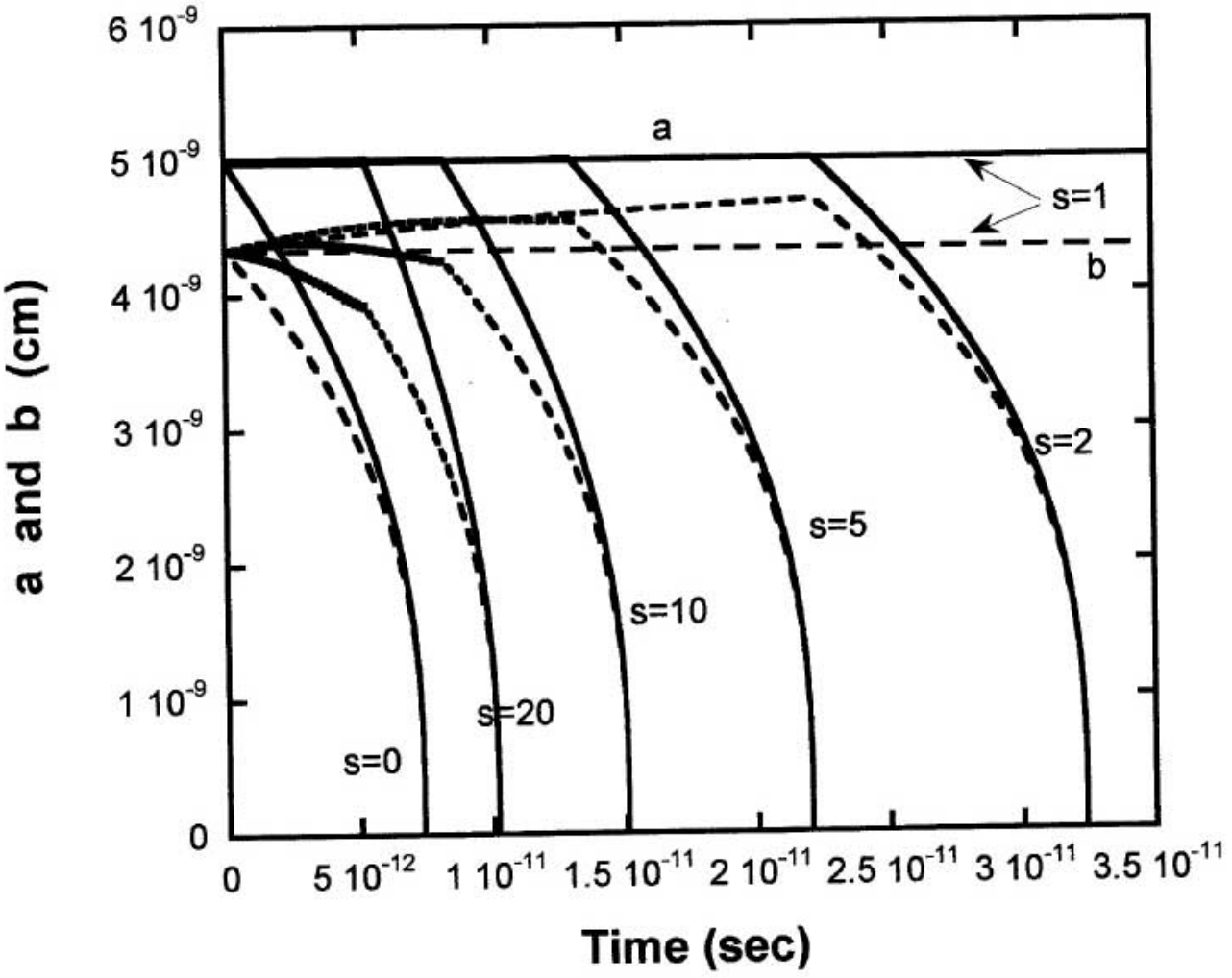

Rydberg Atom Simulation

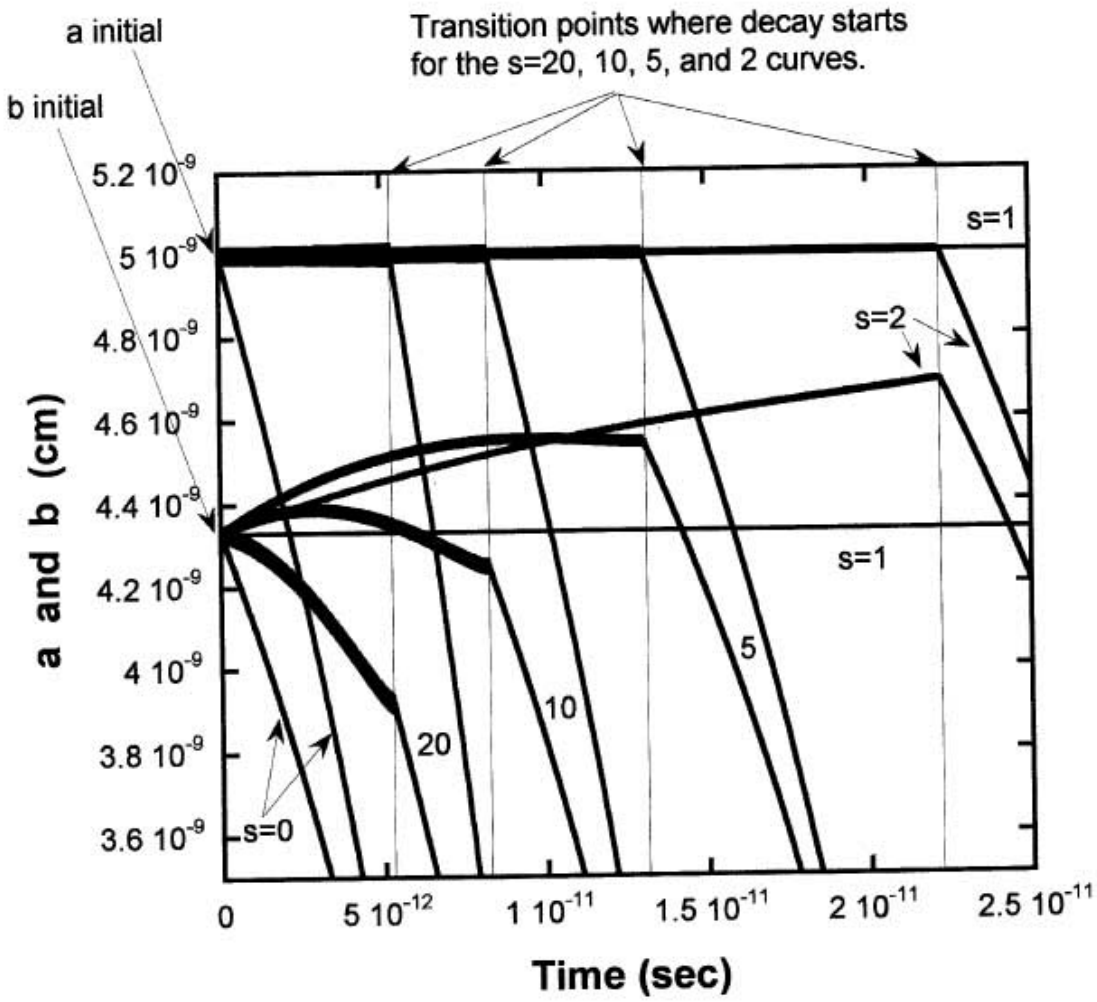

Rydberg Atom Simulation

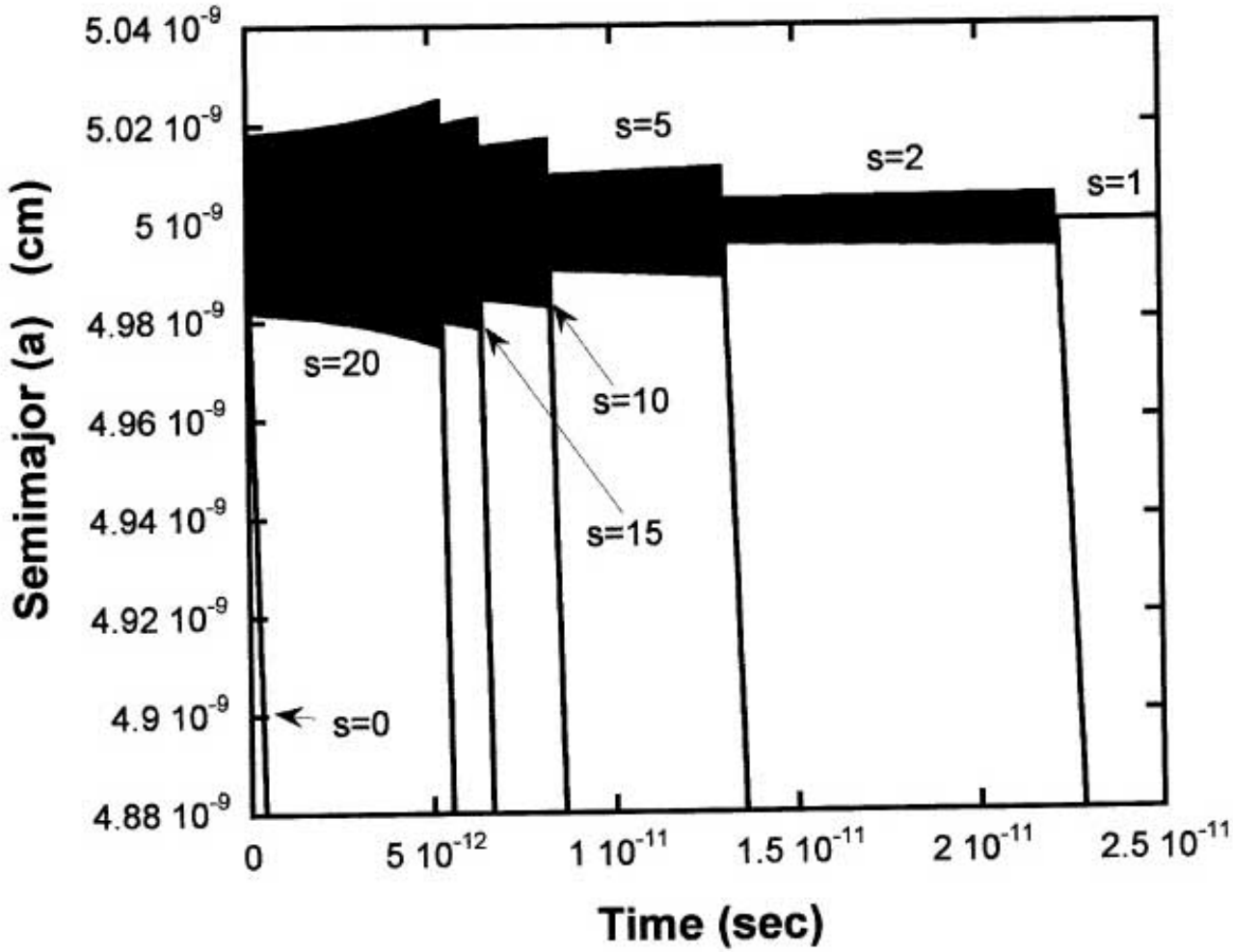

Rydberg Atom Simulation

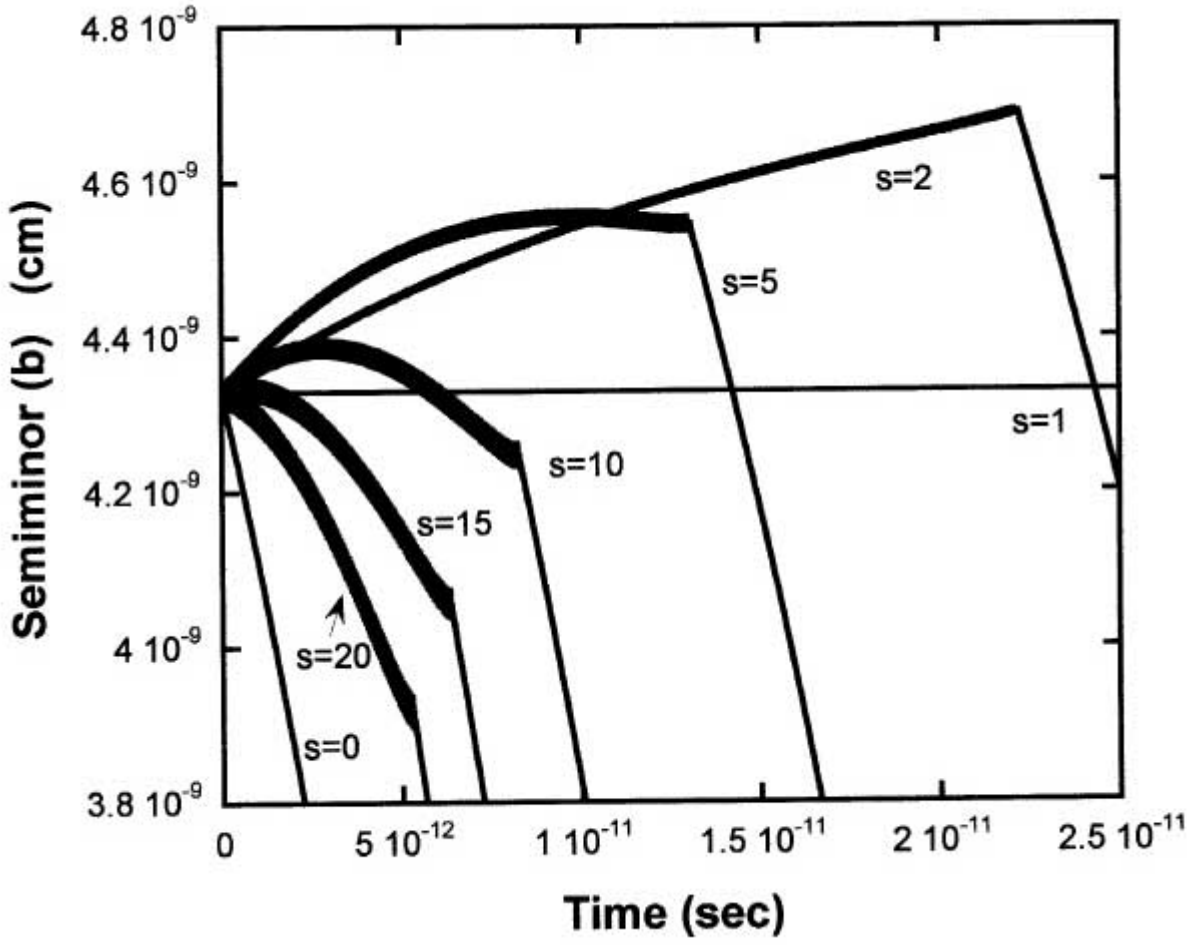

Rydberg Atom Simulation

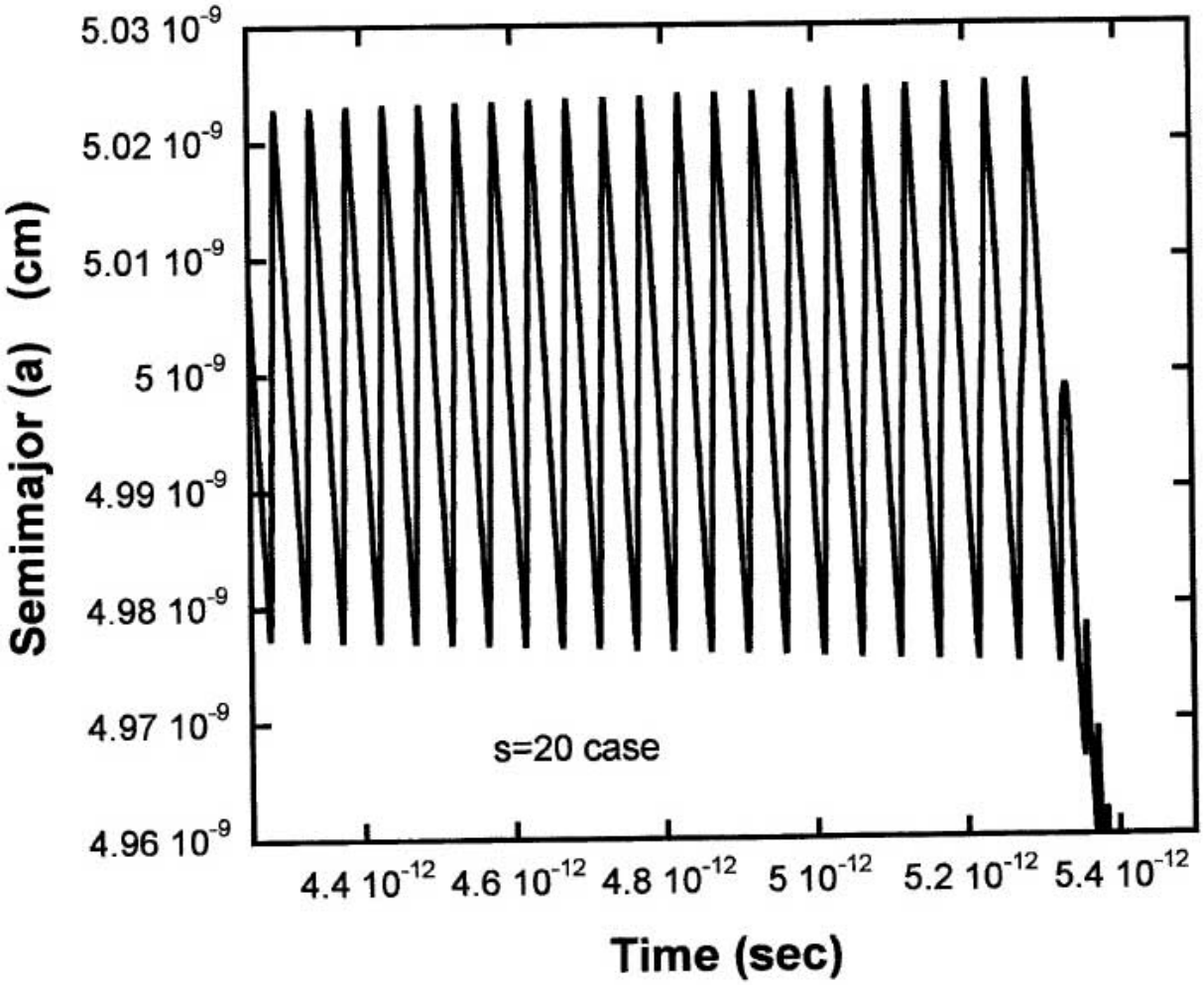

Rydberg Atom Simulation

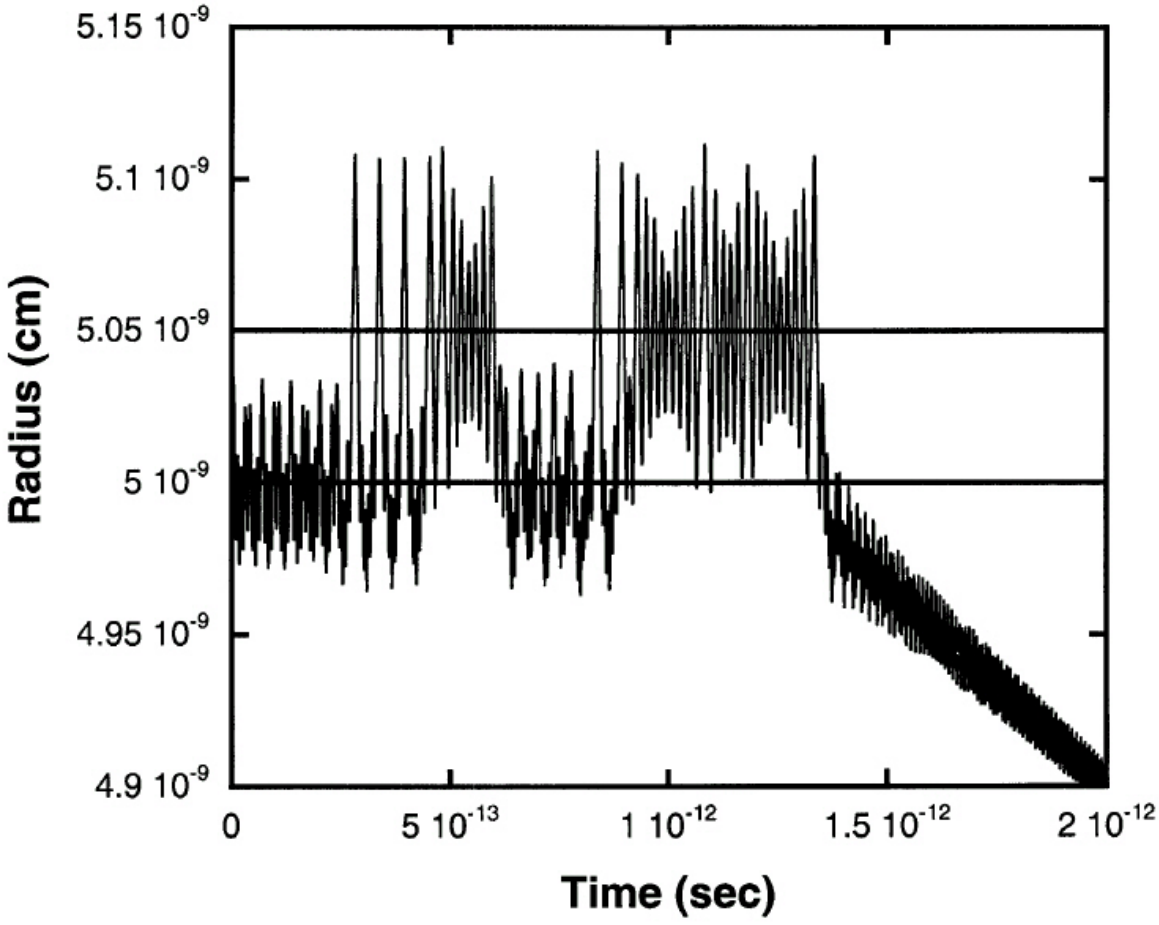

Approximately four “jumps” over about 10,000 orbits.

Rydberg Atom Simulation

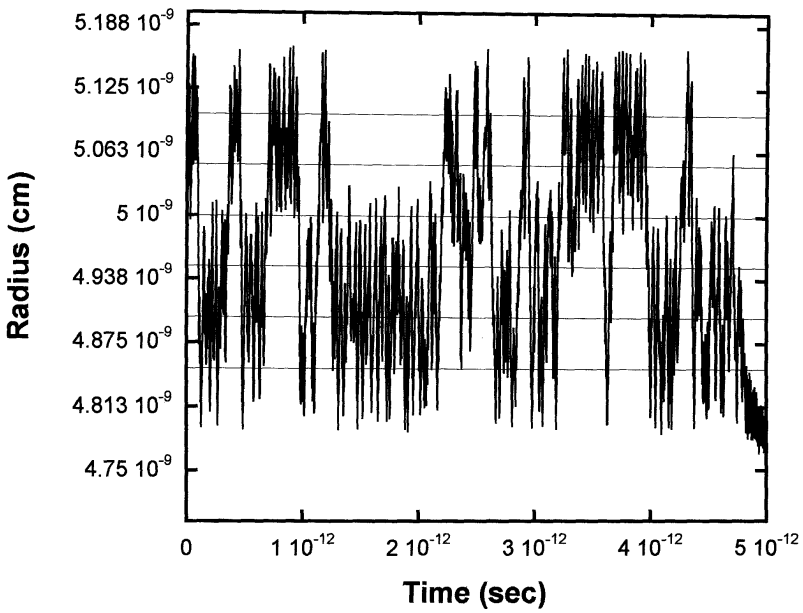

Example of multiple "jumps" .
Note: approximately 36,000 orbits.

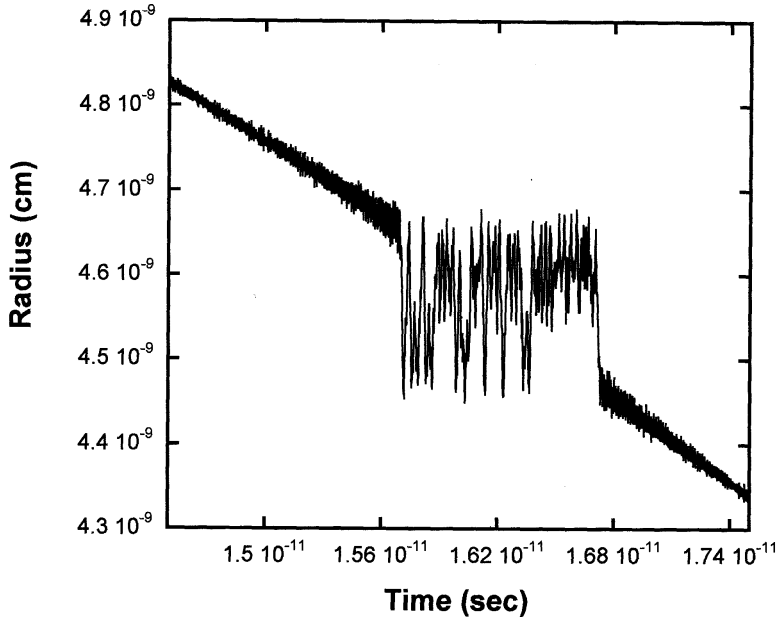

"Catching" an electron
for about 15,000 orbits.

Rydberg Atom Simulation

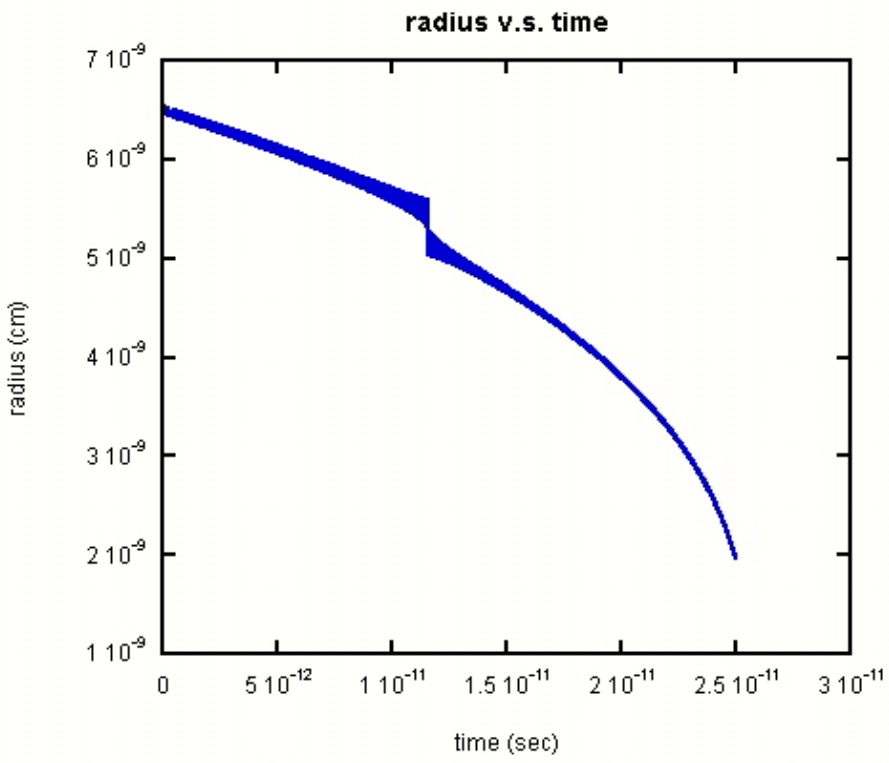

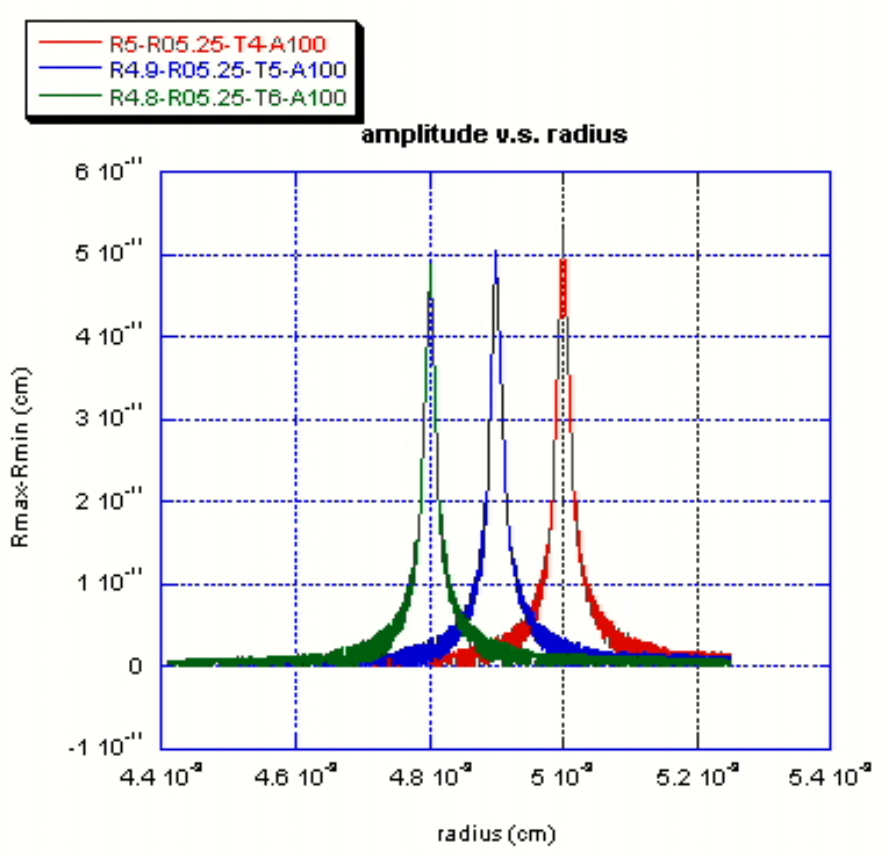

Rydberg Atom Analysis

- **Interesting nonlinear behavior revealed.**
- **Far larger range of "stability" than most people expected.**
- **What happens if we go to the next level, and examine radiation and the atom in a possible "thermodynamic equilibrium" ?**

Classical Electromagnetic Zero-Point (ZP) Radiation

- Key part of the theory called "Stochastic Electrodynamics". To provide thermodynamic equilibrium, the interaction of charged particles and electromagnetic fields must be carefully taken into account.

- ZP radiation: spectrum at temperature $T=0$. Some properties:
  - Only spectrum that is Lorentz invariant
  - Only spectrum that provides no "heat flow" during reversible thermodynamic operations.

$$\rho_{\mathrm{ZP}}(\omega)=\frac{\hbar\omega^3}{2\pi^2} \quad , \quad \frac{1}{8\pi}\left\langle \mathbf{E}^2+\mathbf{B}^2\right\rangle_{\mathrm{ZP}}=\int_0^\infty d\omega\rho_{\mathrm{ZP}}(\omega)$$

Rydberg Atom Simulation

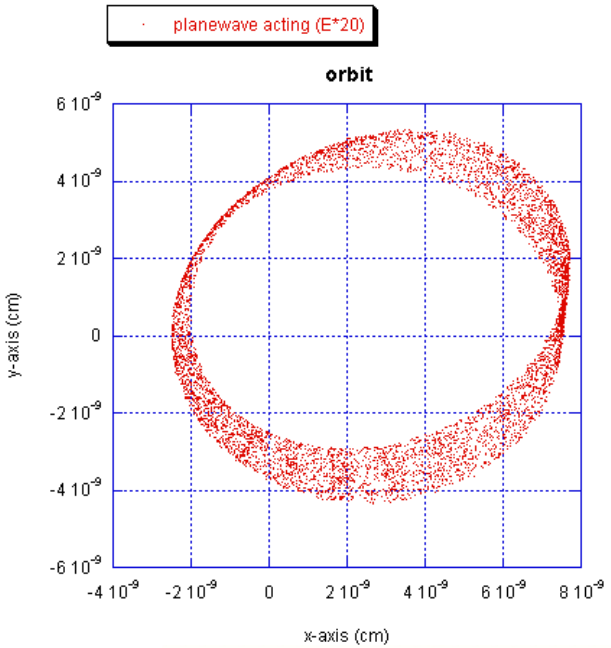

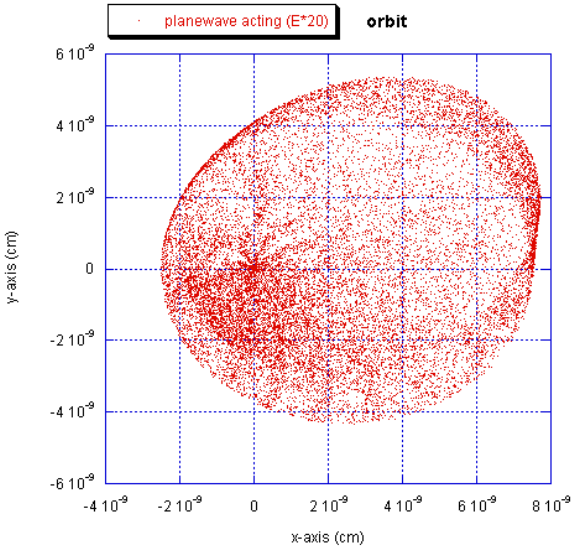

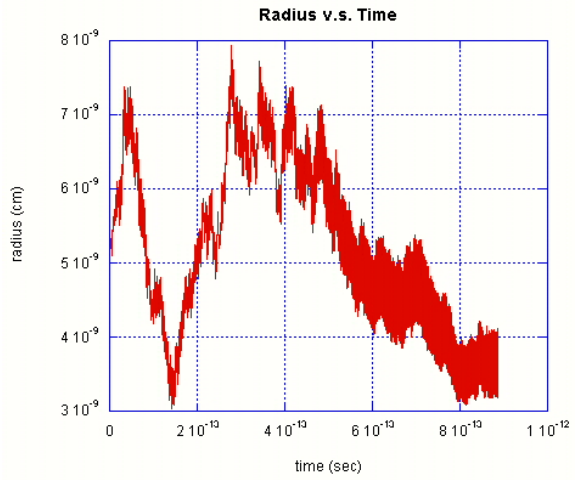

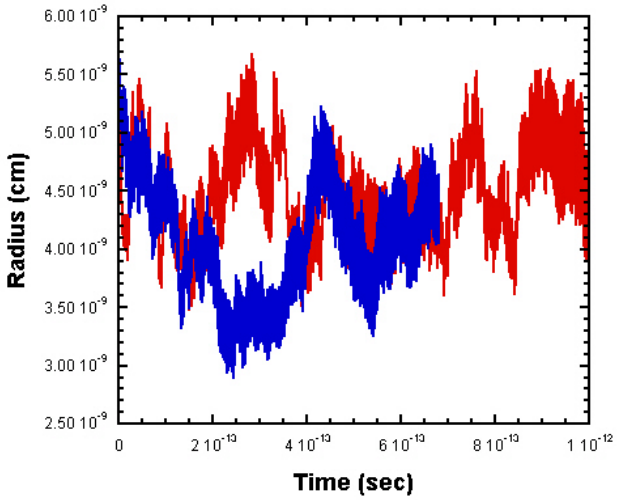

Rydberg Atom Simulation

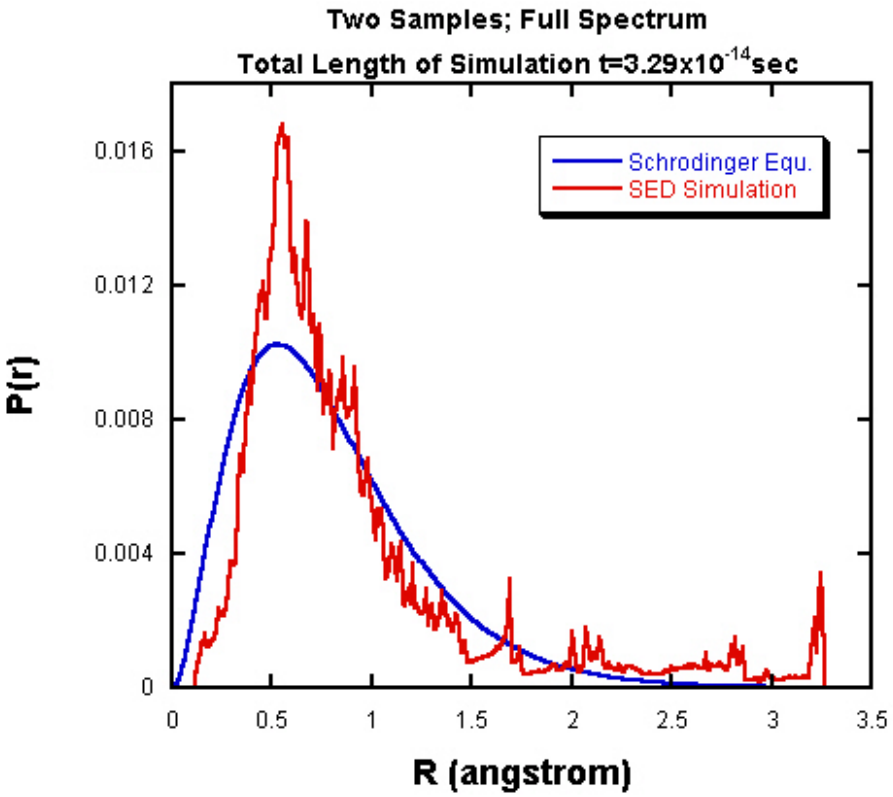

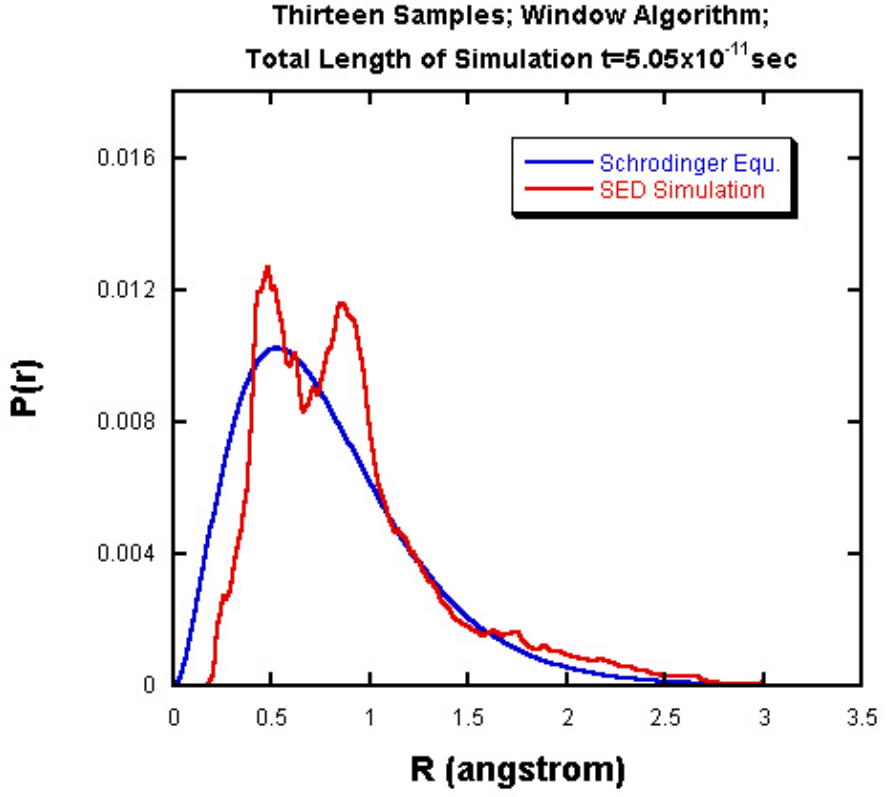

Rydberg Atom Simulation

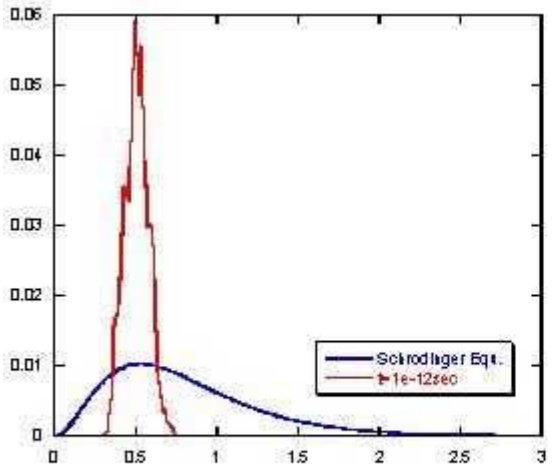

t=1.0e-12sec

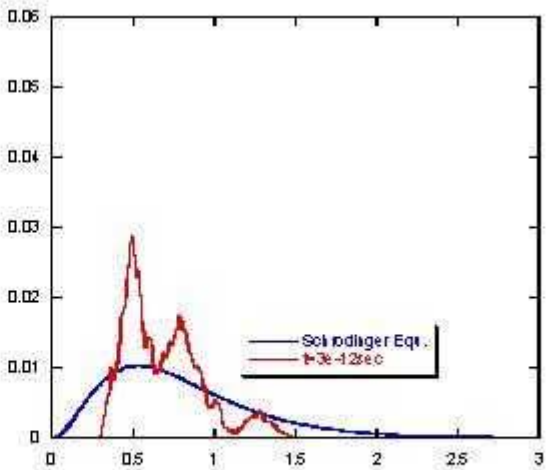

t=3.0e-12sec

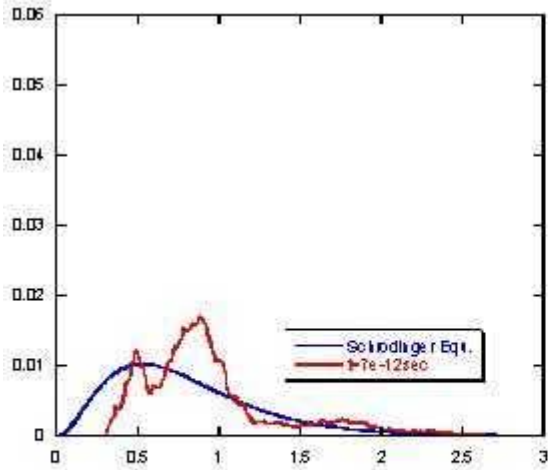

t=7.0e-12sec

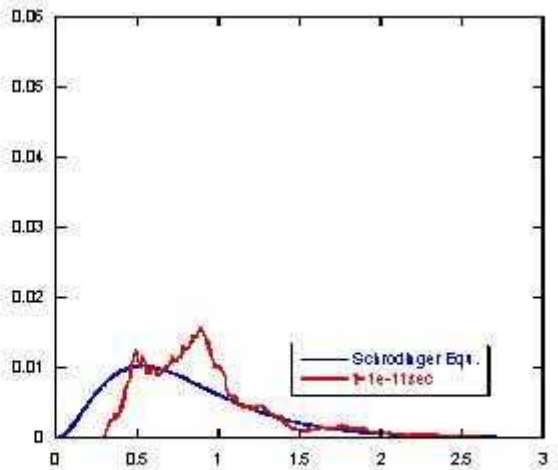

t=1.0e-11sec

Rydberg Analysis

"Simulation Study of Aspects of the Classical Hydrogen Atom Interacting with Electromagnetic Radiation: Circular Orbits," by D. C. Cole and Y. Zou. To be published in Journal of Scientific Computing, Vol. 18, No. 3, June 2003.

"Simulation Study of Aspects of the Classical Hydrogen Atom Interacting with Electromagnetic Radiation: Elliptical Orbits," by D. C. Cole and Y. Zou. To be published in Journal of Scientific Computing, 2003.

"Analysis of Orbital Decay Time for the Classical Hydrogen Atom Interacting with Circularly Polarized Electromagnetic Radiation," by D. C. Cole and Y. Zou, submitted to J. Computational Physics.

"Perturbation Analysis and Simulation Study of the Effects of Phase on the Classical Hydrogen Atom Interacting with Circularly Polarized Electromagnetic Radiation," by D. C. Cole and Y. Zou, submitted to J. Computational Physics.

Earlier related articles on SED published in Physical Review (9 articles) and Foundations of Physics (4 articles)

Rydberg Atom Simulation

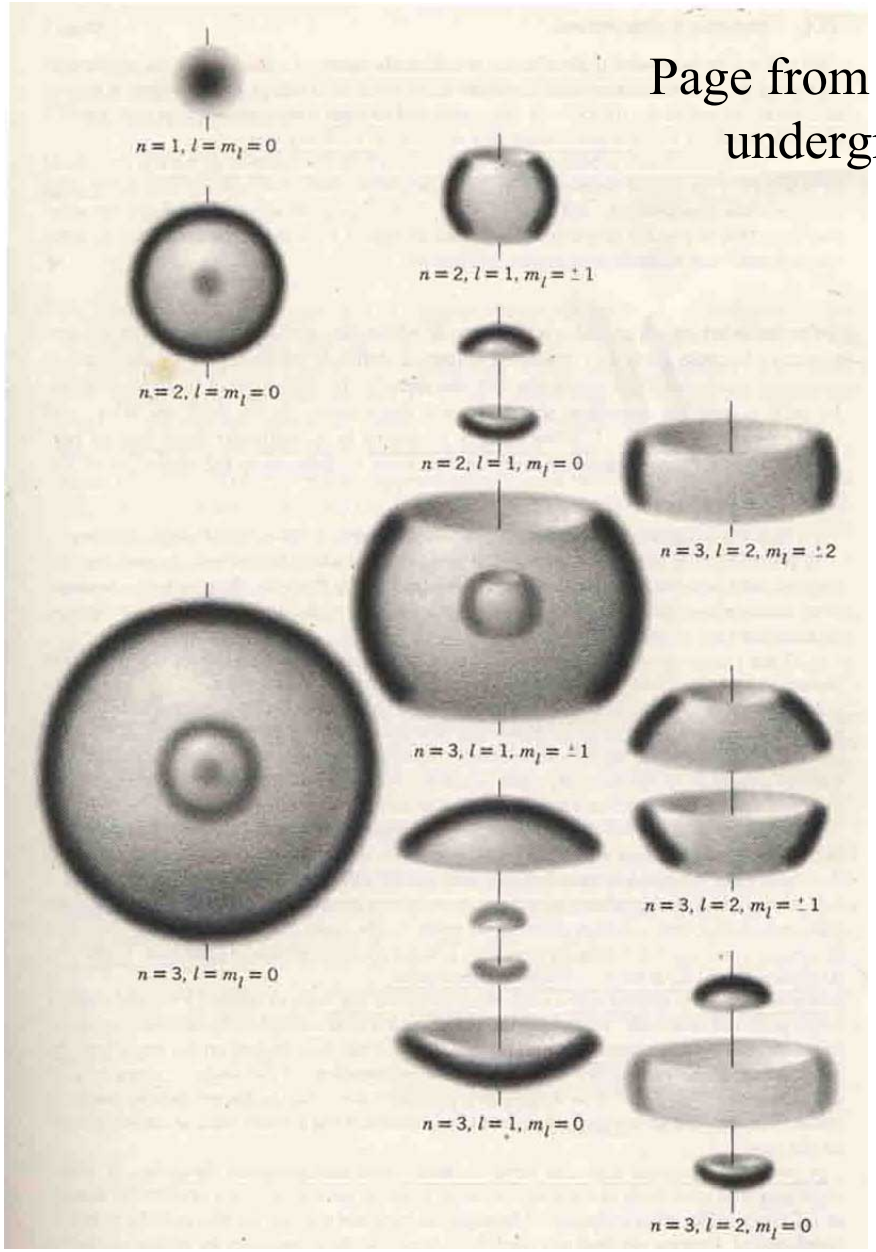

Page from Eisberg's and Renick's undergraduate text on QM.

(Backup slide)

Rydberg Atom Simulation

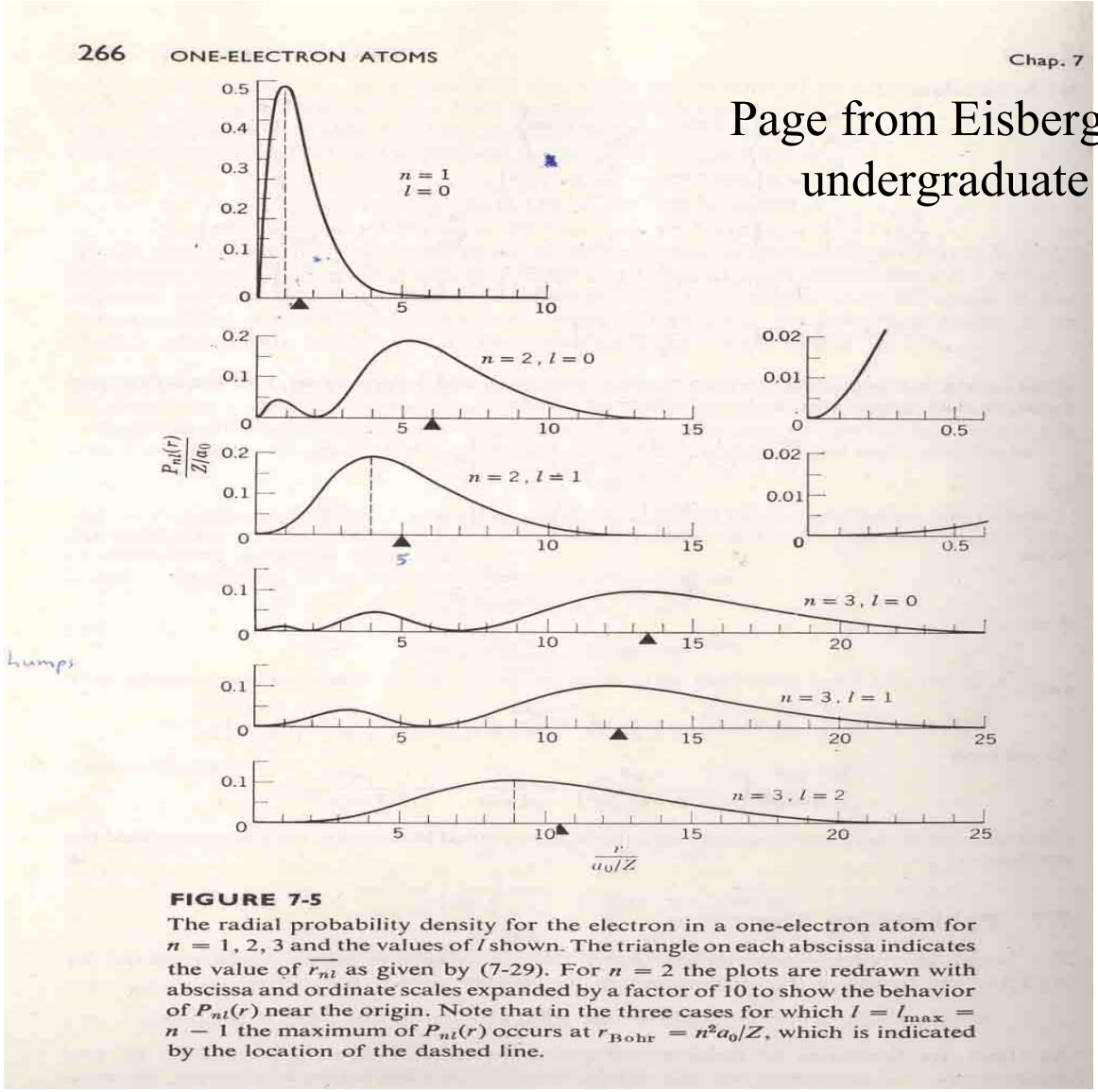

FIGURE 7-5
The radial probability density for the electron in a one-electron atom for $n = 1, 2, 3$ and the values of l shown. The triangle on each abscissa indicates the value of $\overline{r_{nl}}$ as given by (7-29). For $n = 2$ the plots are redrawn with abscissa and ordinate scales expanded by a factor of 10 to show the behavior of $P_{nl}(r)$ near the origin. Note that in the three cases for which $l = l_{max} = n - 1$ the maximum of $P_{nl}(r)$ occurs at $r_{Bohr} = n^2 a_0/Z$, which is indicated by the location of the dashed line.

Page from Eisberg's and Renick's undergraduate text on QM.

(Backup slide)

For a situation like this, the survival probability $P_{\rm surv}$, i.e. the probability to find the atom in a bound state after an atom-field interaction time $t = t_2 - t_1$, writes:

$$P_{\rm surv}(t_2 - t_1) = \sum_{\text{bound states } |\xi_m\rangle} \left|\langle \xi_m | U(t_2, t_1) | n_0, \ell_0, m_0 \rangle\right|^2, \quad \text{(Backup slide)}$$

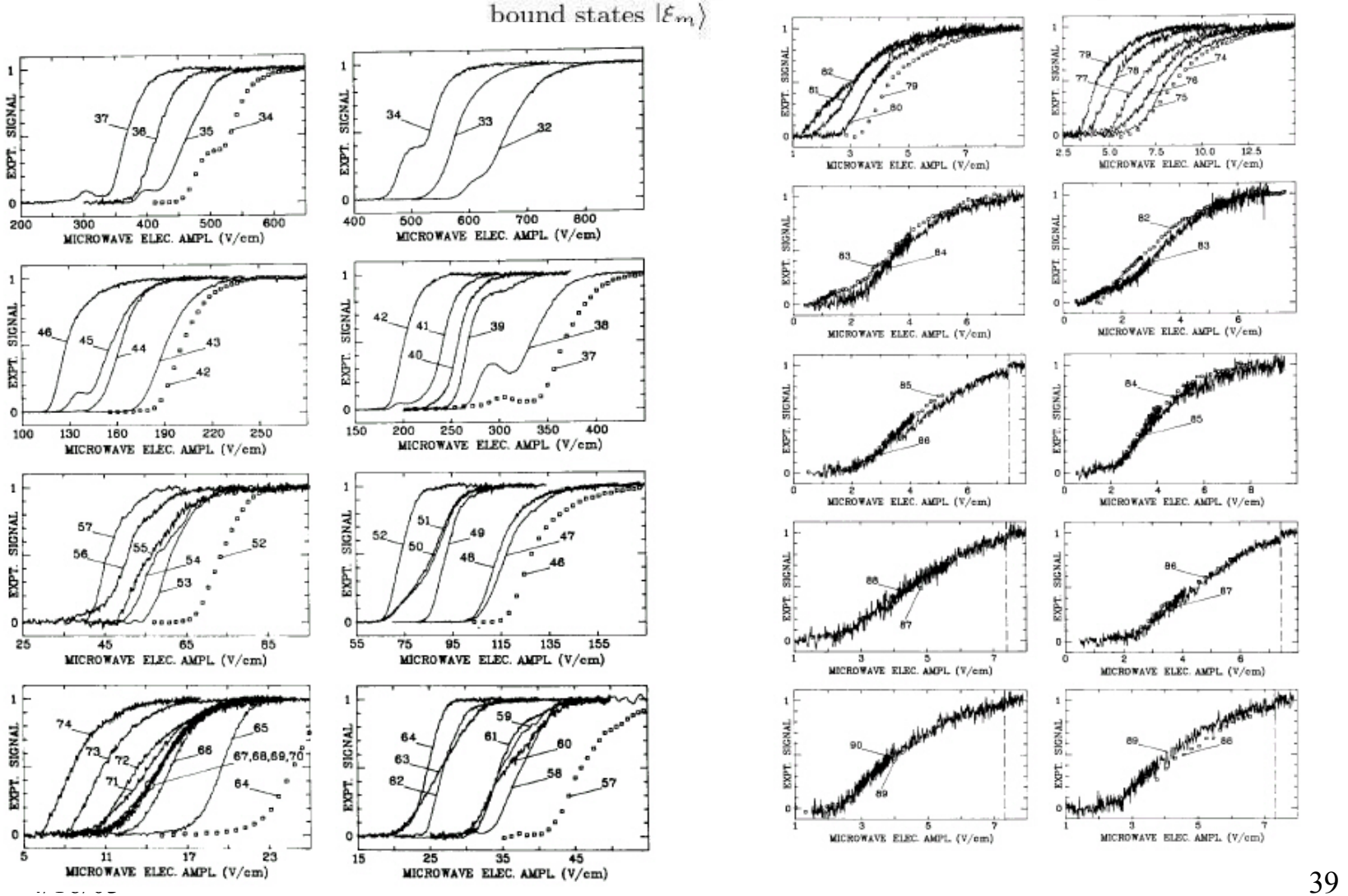

Ionization probability (experimental data) from Koch's 1995 review article.

Microlithography: Photoresist bias model.

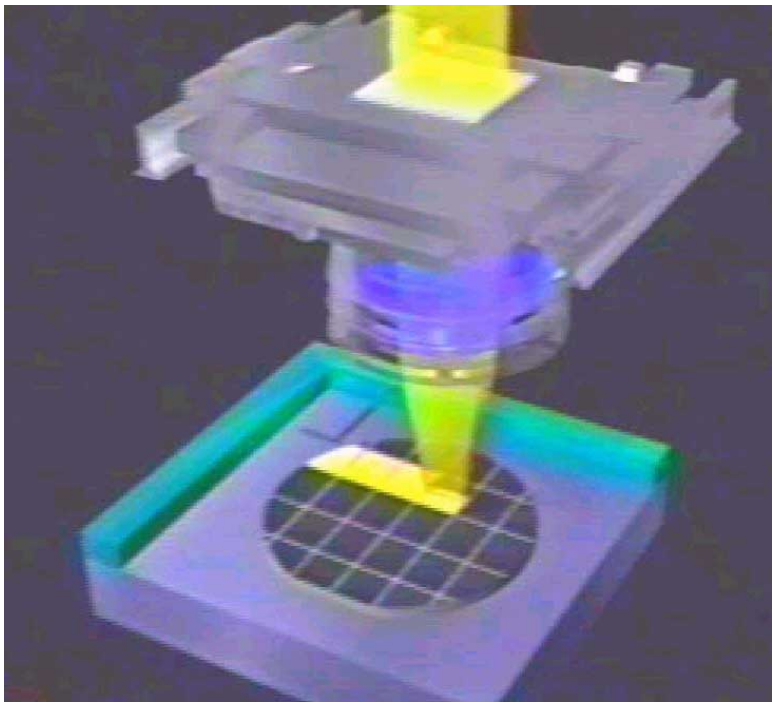

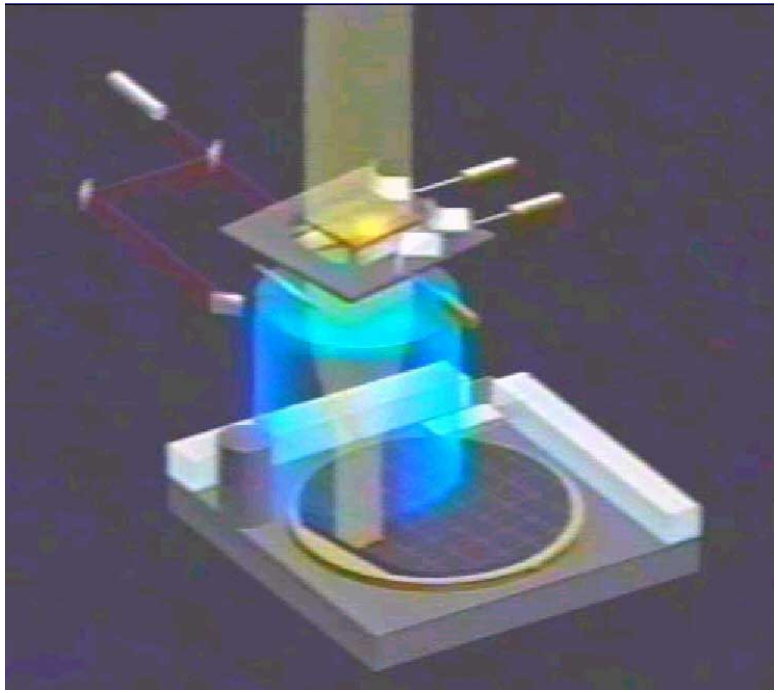

$$I(\mathbf{x}_O) = \int_{\text{Mask}} d^2x \int_{\text{Mask}} d^2x' K(\mathbf{x}_I, \mathbf{x}_O) K^*(\mathbf{x}_I, \mathbf{x}'_O) T(\mathbf{x}_O) T^*(\mathbf{x}'_O) J(\mathbf{x}_O, \mathbf{x}'_O)$$

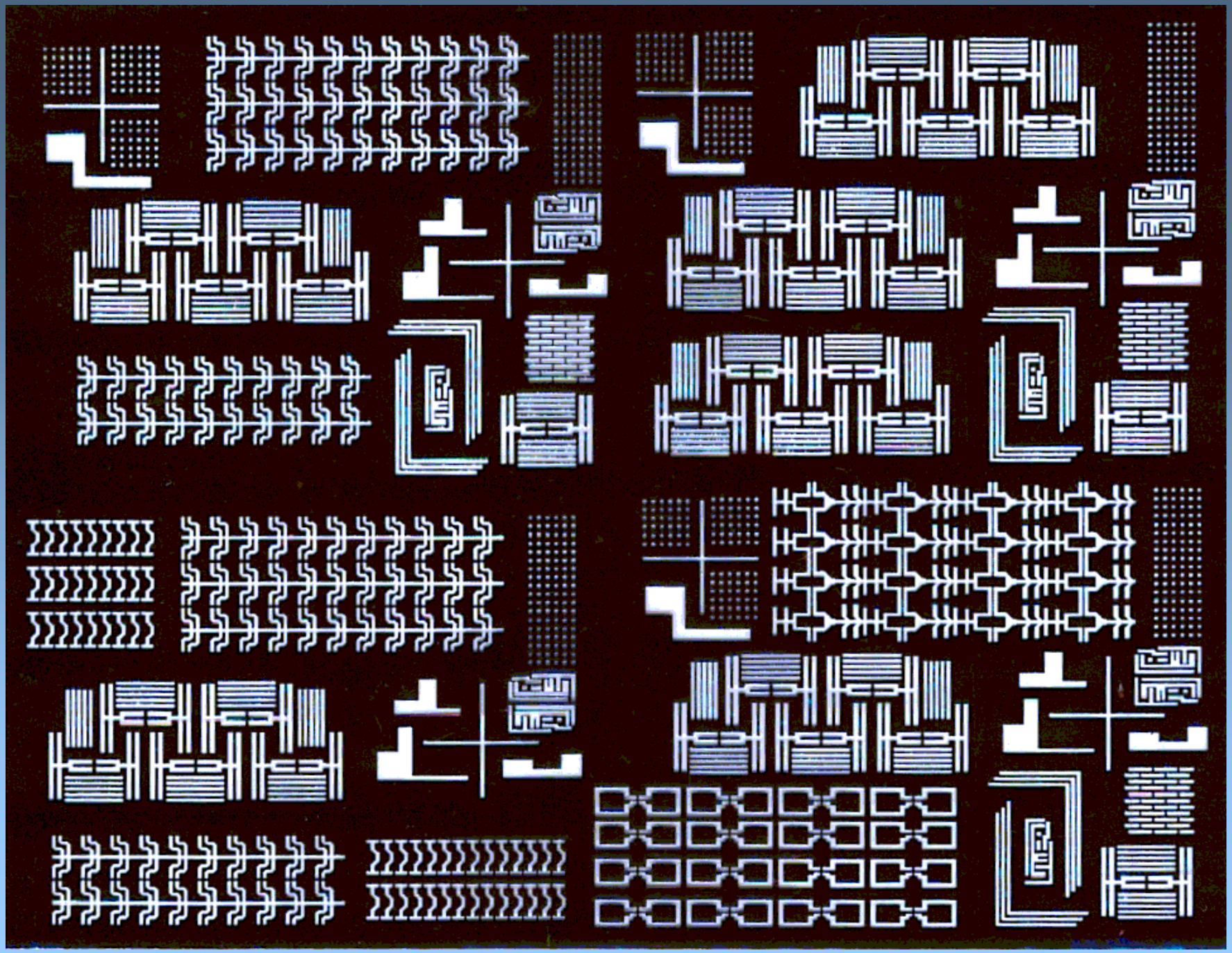

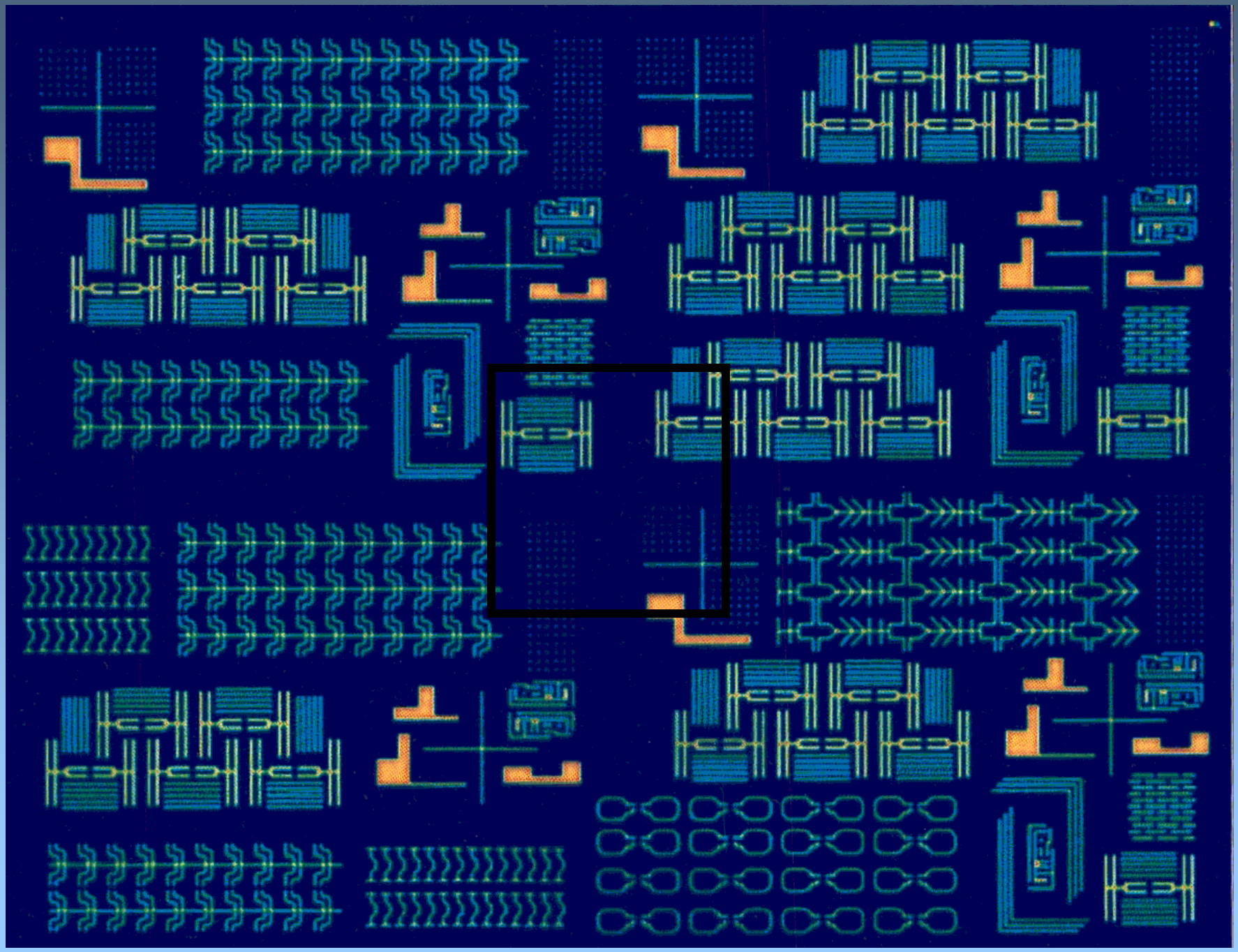

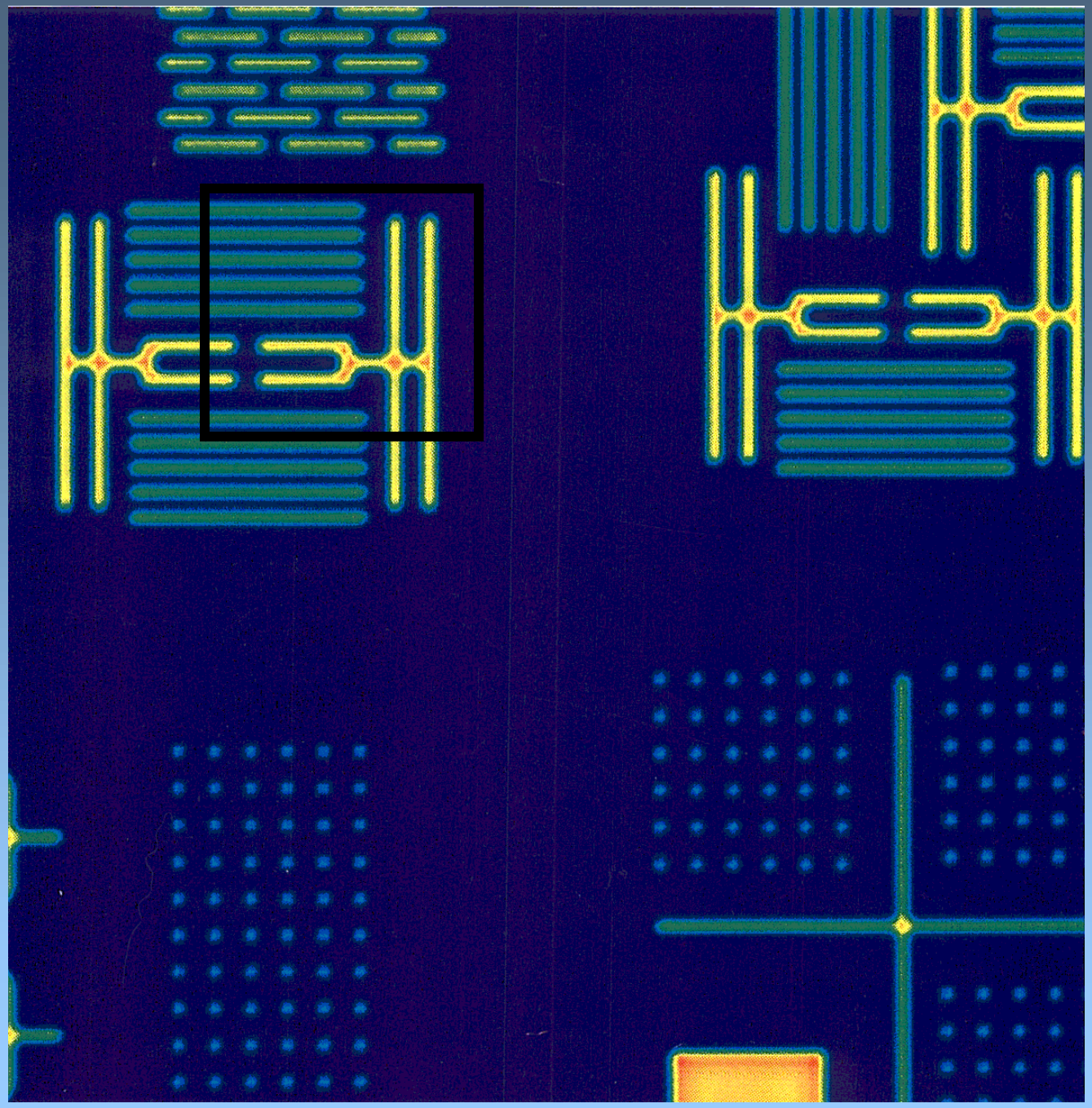

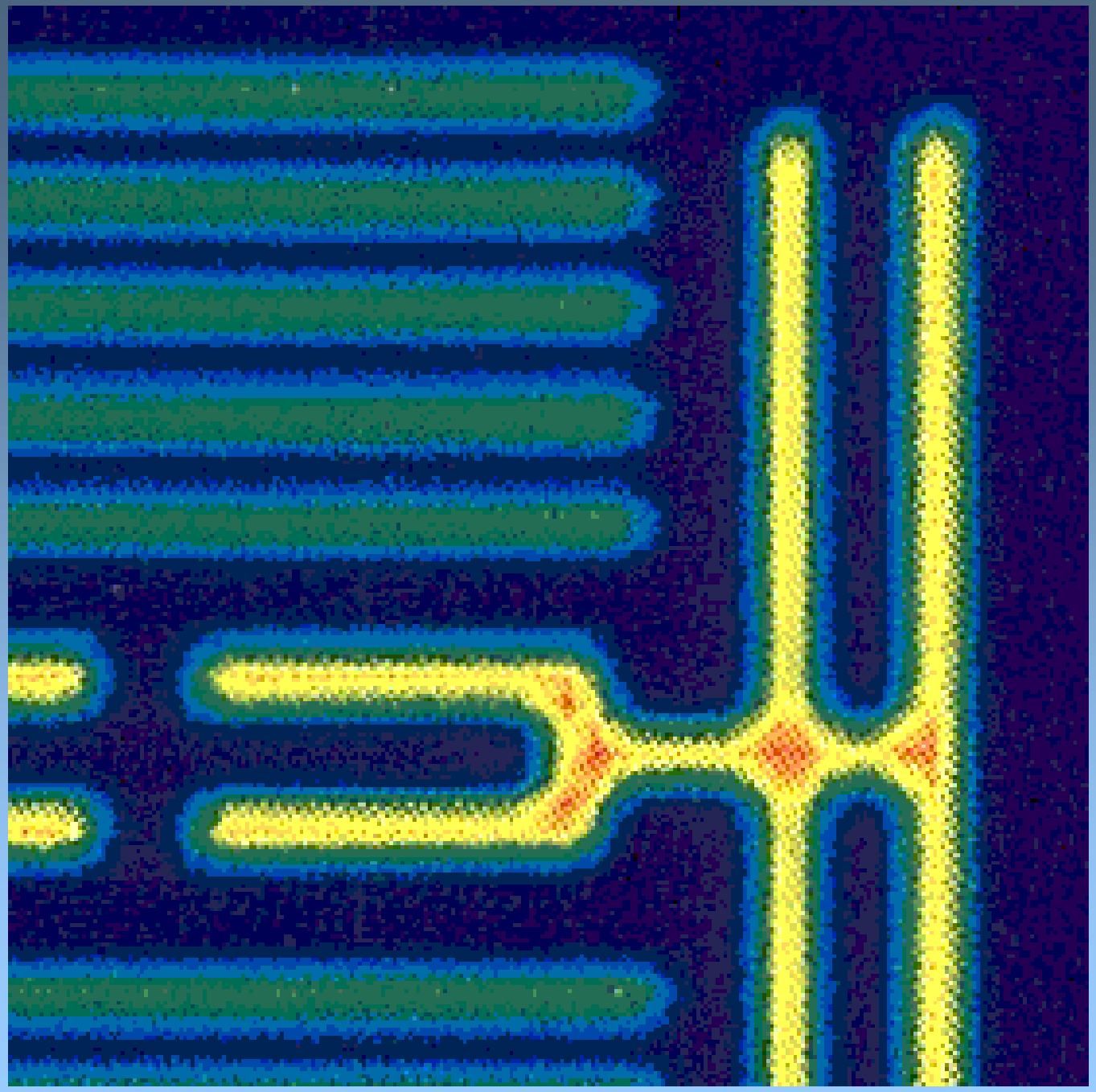

Superposition of predictions from (1) a threshold aerial image model (outside curve), (2) threshold aerial image model with mask corrections (middle curve), (3) diffused aerial image threshold model, with mask corrections (outside curve).

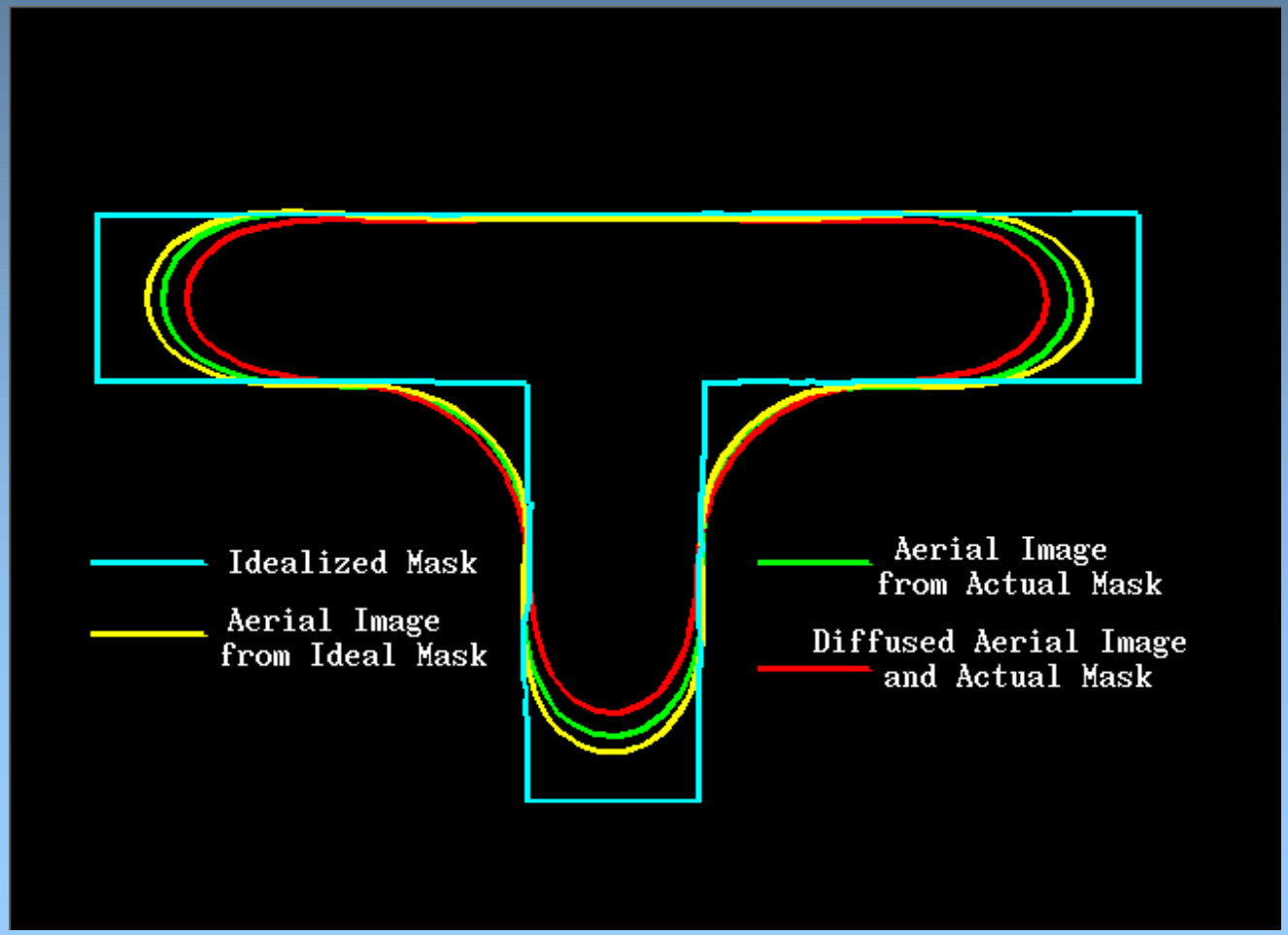

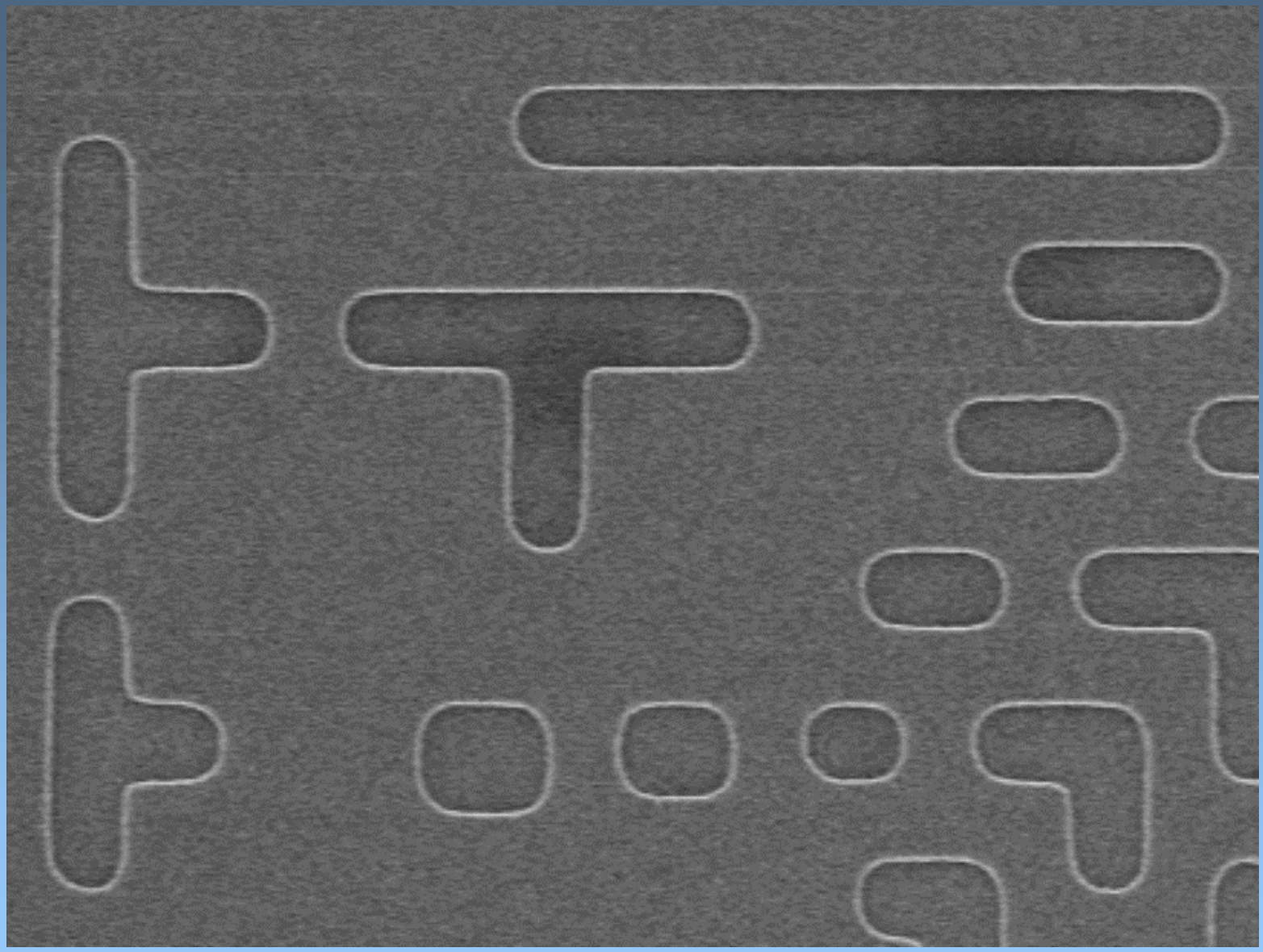

Fig. 1: SEM micrograph of an optical projection reticle. Smallest size is 0.25 um on wafer, 1.0 um on mask (4X).

SEM of UV2HS photoresist structures, corresponding to the mask pattern shown in Fig. 1. The nominal focus setting used here was 0.0 um from the Gaussian image plane.

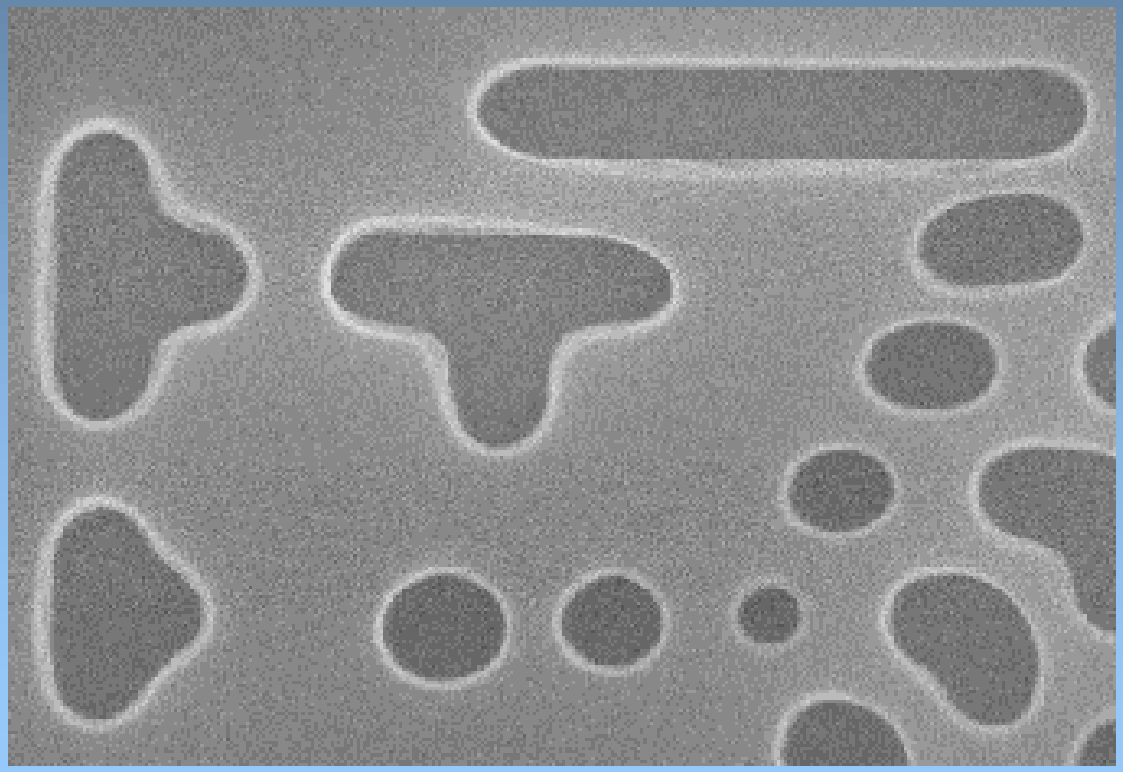

Fig. 3: SEM of UV2HS photoresist structures, corresponding to the mask pattern shown in Fig. 1. The nominal focus setting used here was 0.75 um from the Gaussian image plane. Note: the smallest structure on the bottom right of Fig. 1 does not print at this defocus condition.

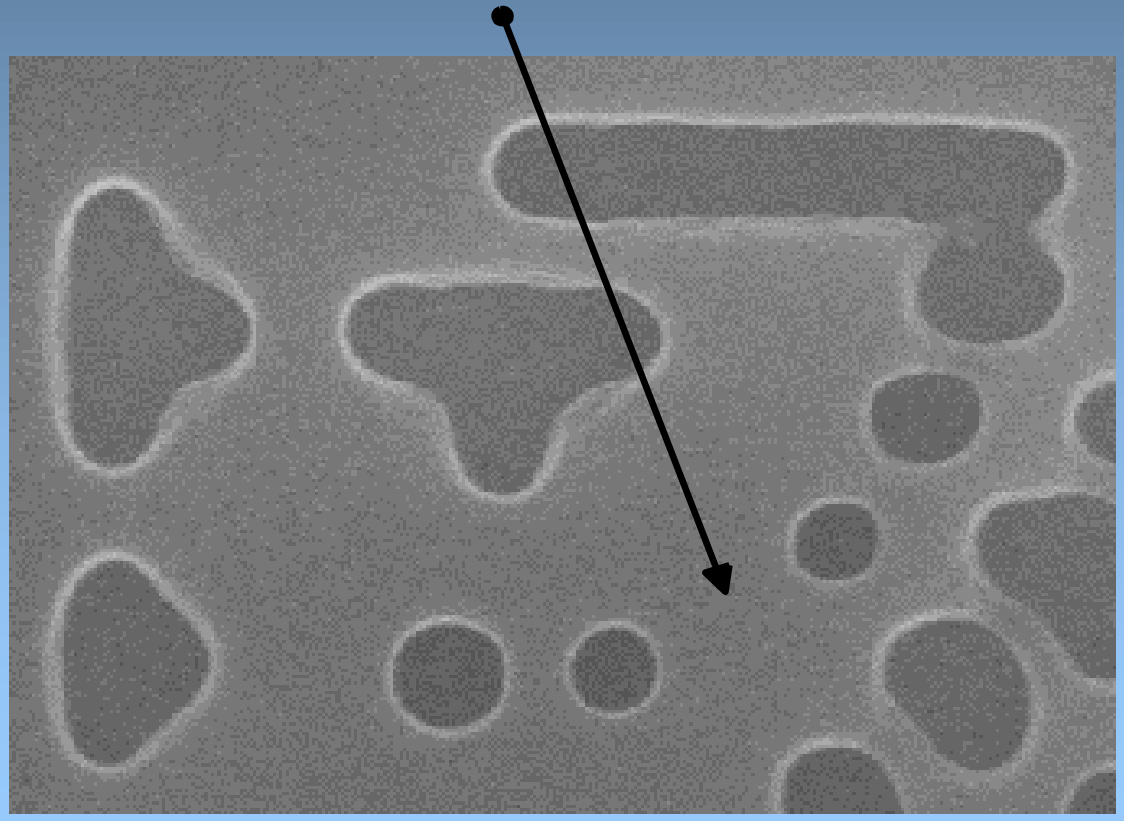

Vector plot of the deviations between simulation and SEM measurements corresponding to one of the UV2HS printed "T" shapes in Fig. 1. Note: maximum deviation here is 27 NM.

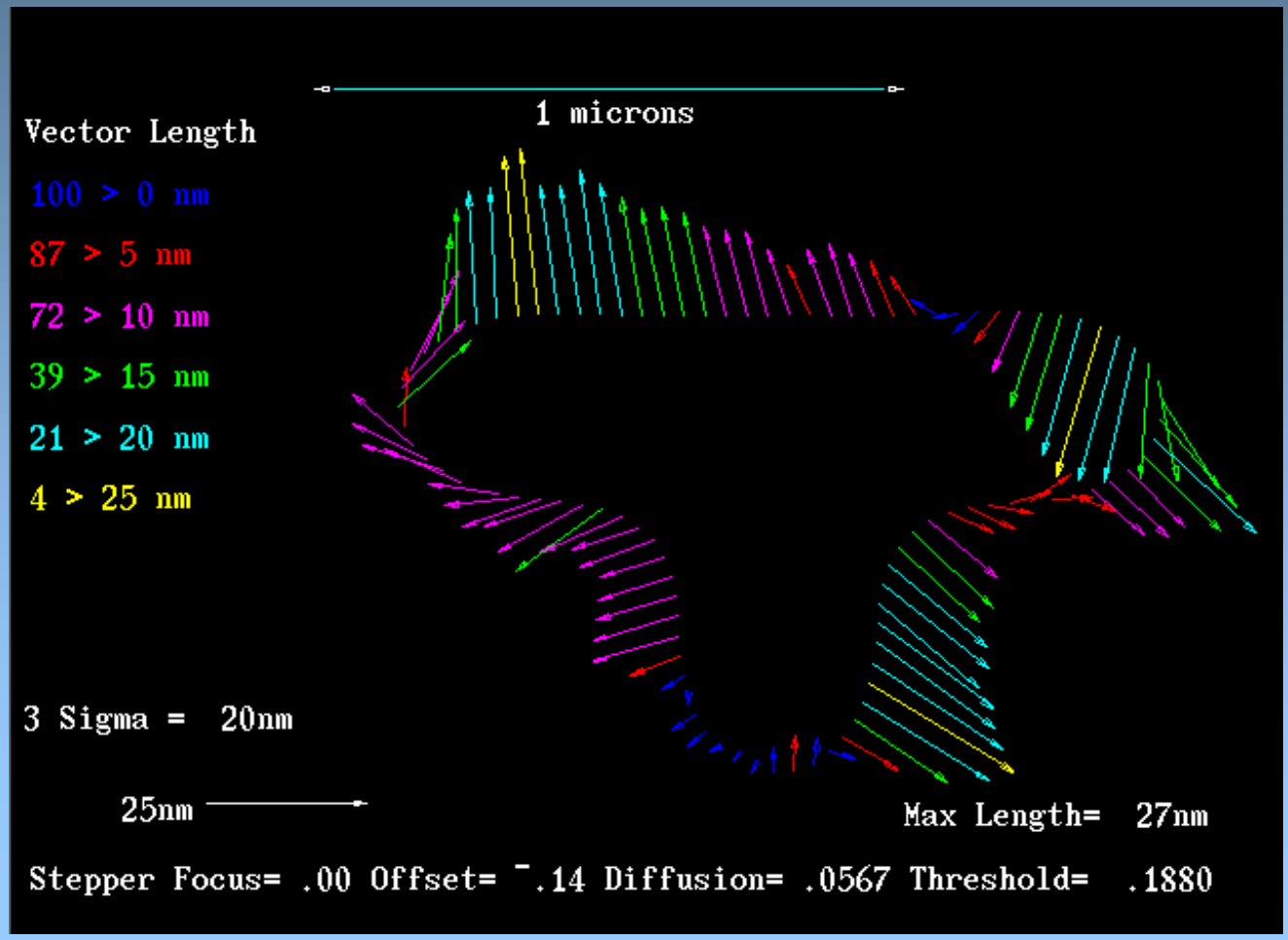

Plot showing differences between the SEM detected edge of the resist structure in Fig. 2 and simulation.

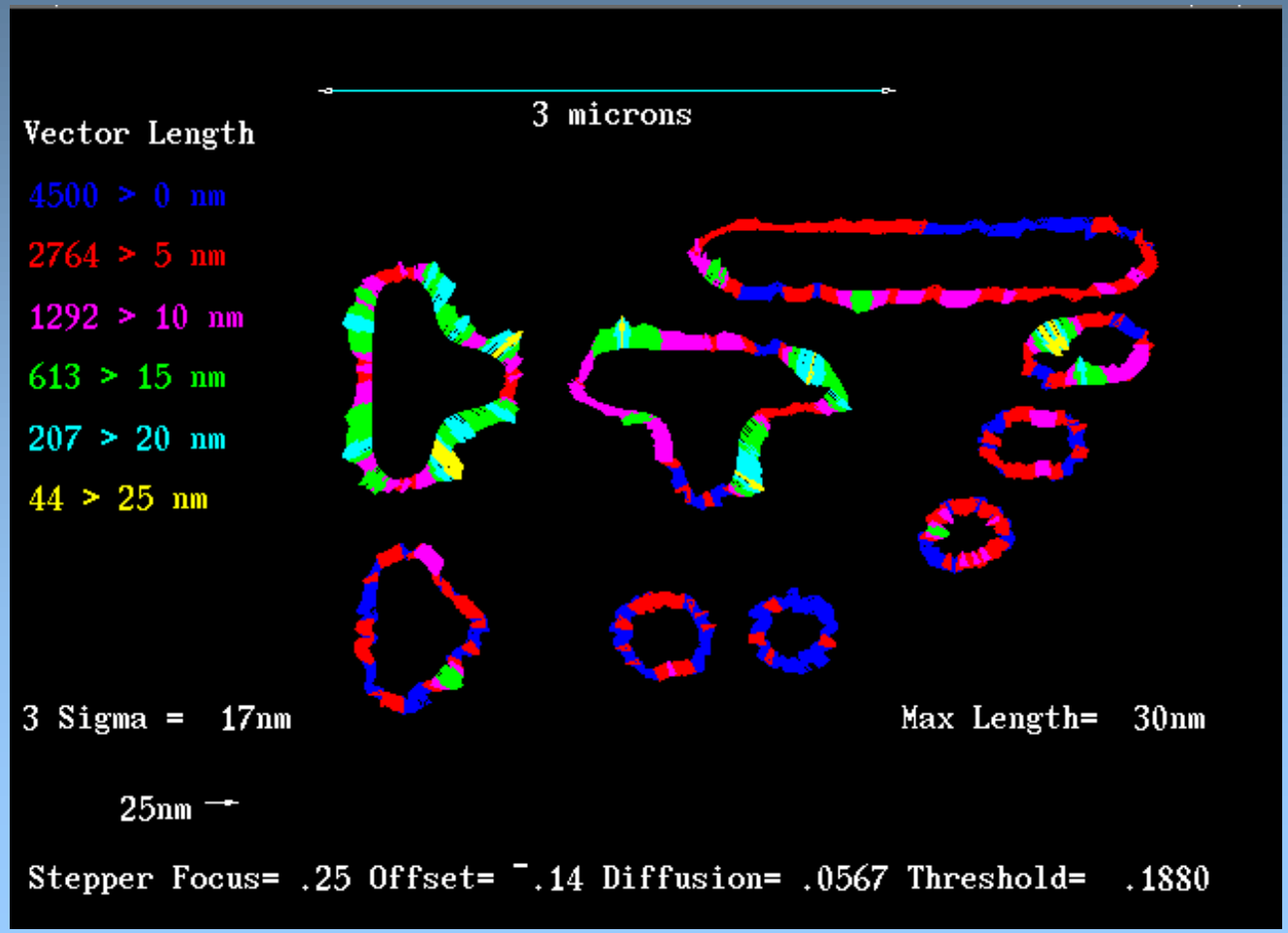

Simulation of Physical Processes

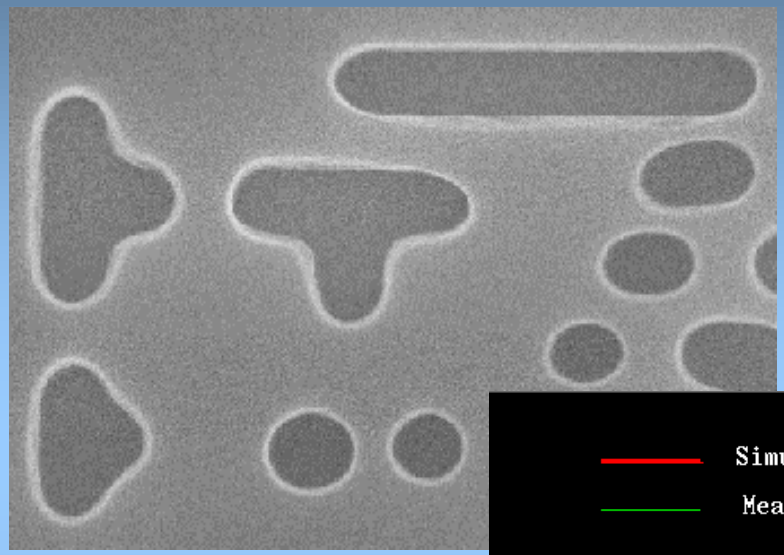

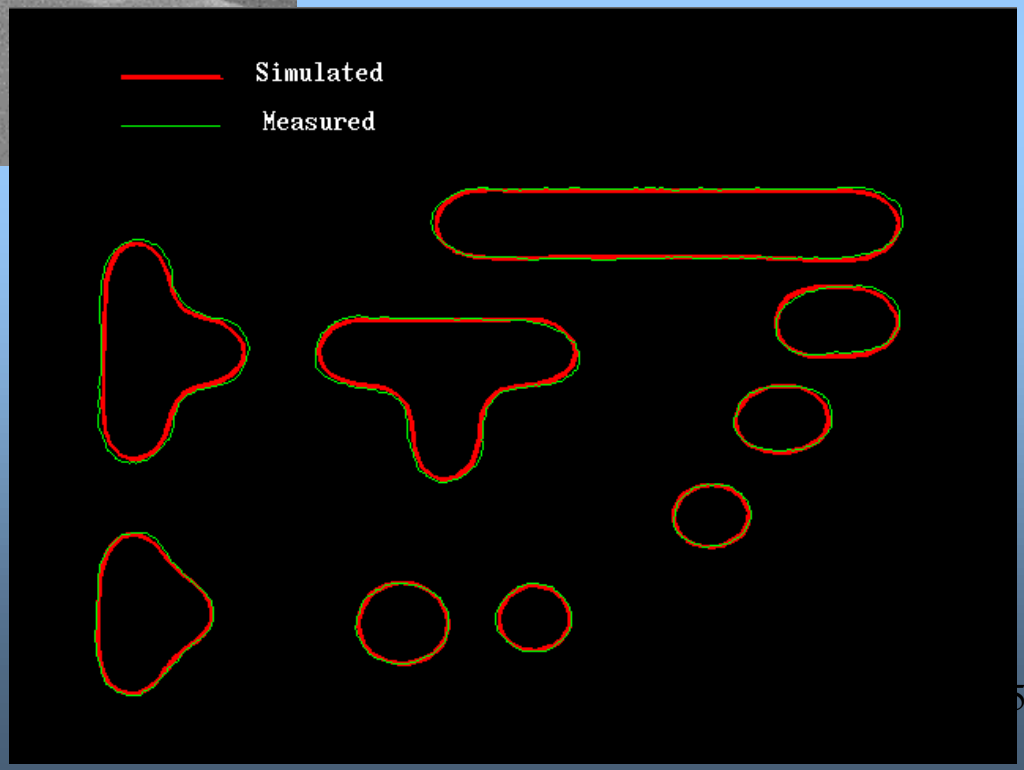

Simulation of Physical Processes

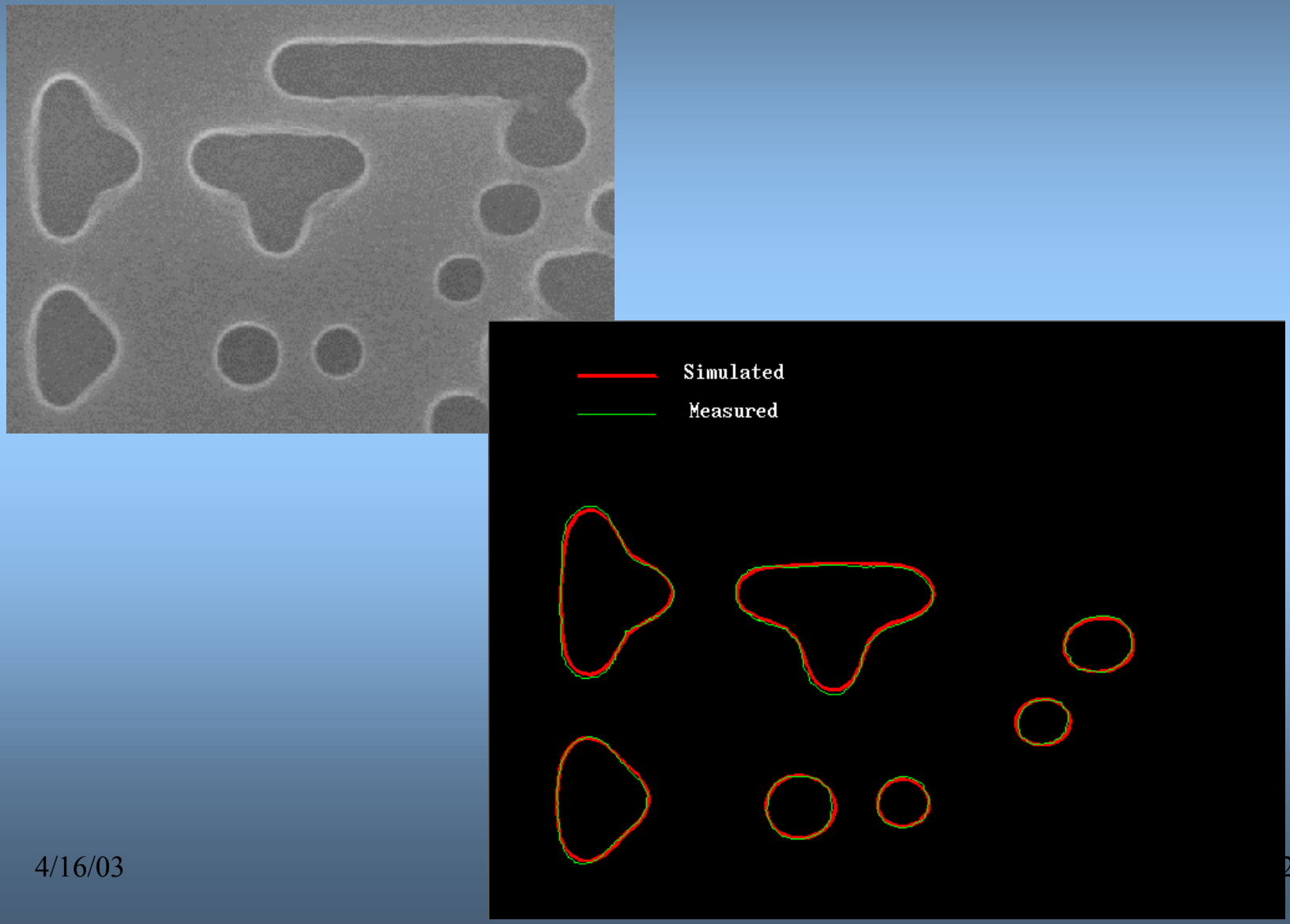

CAD layout of section of SRAM cell. Four design levels of gate, diffusion, contact, and first metal interconnect are superimposed here.

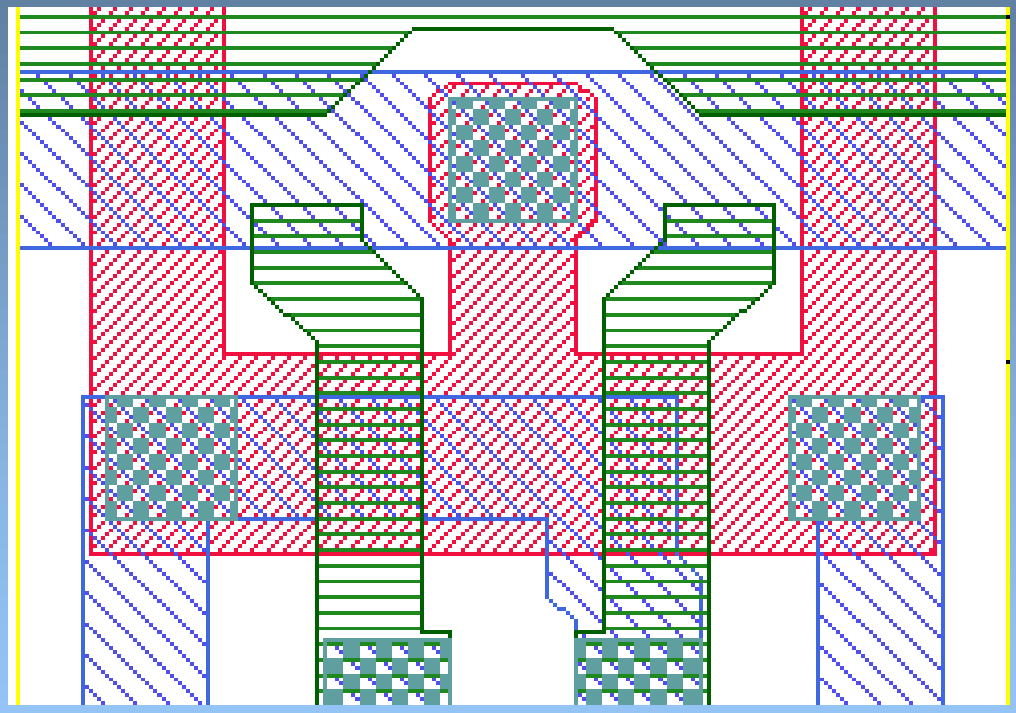

The predicted shapes from the phenomenological resist and etch bias models are shown here for the following levels: gate, diffusion, contact, and first metal interconnect. The predicted shapes are overlaid with the original CAD design.

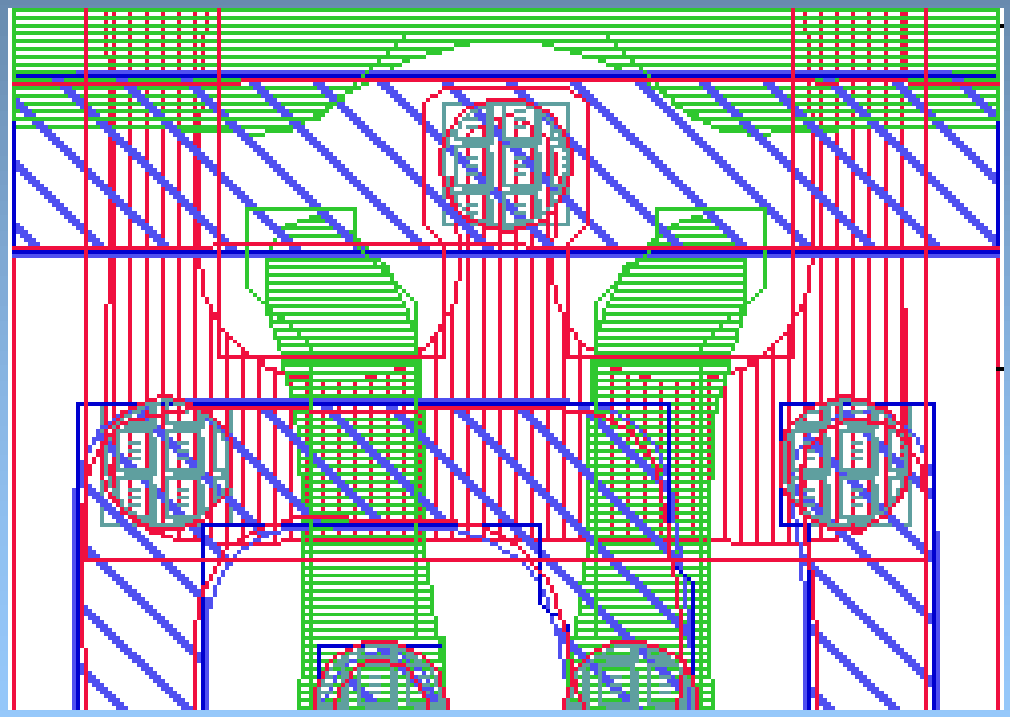

Simulation of Physical Processes

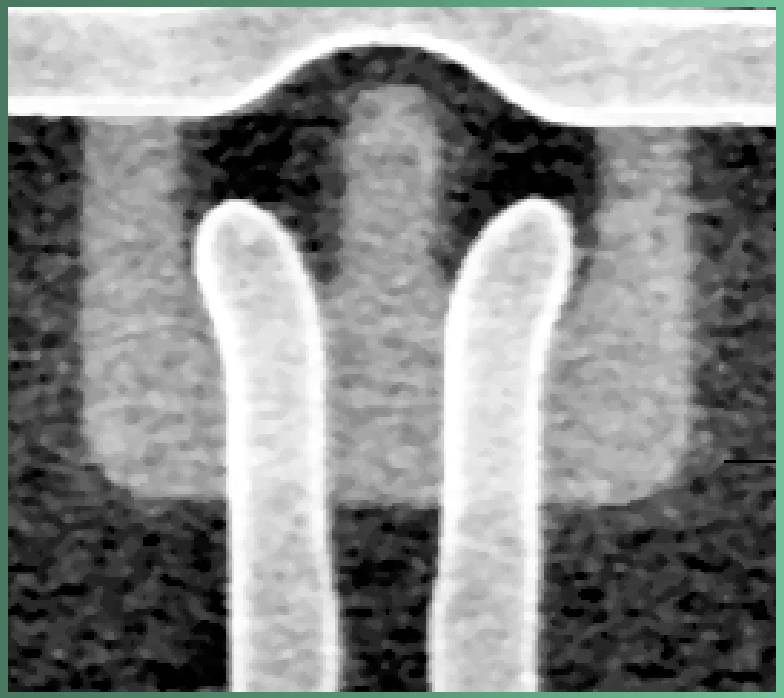

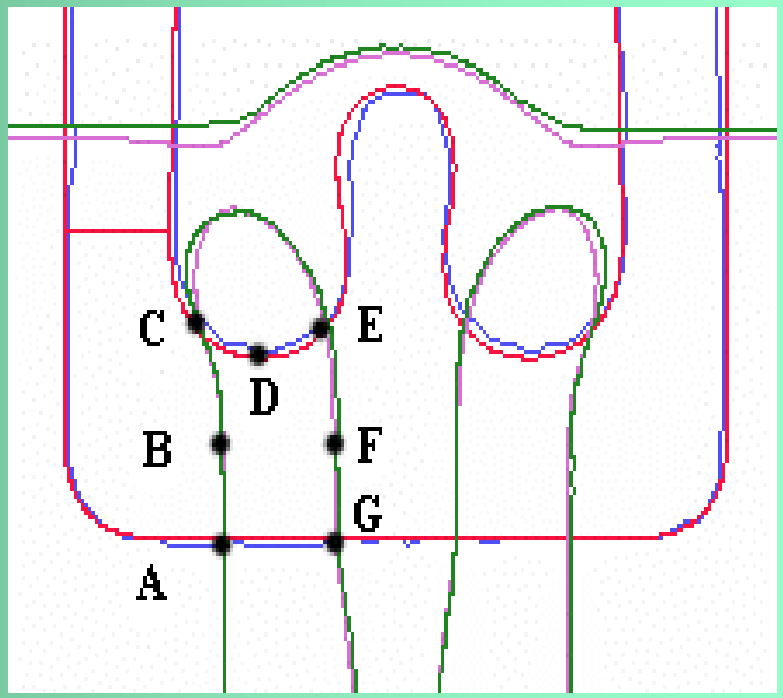

Simulation of Physical Processes

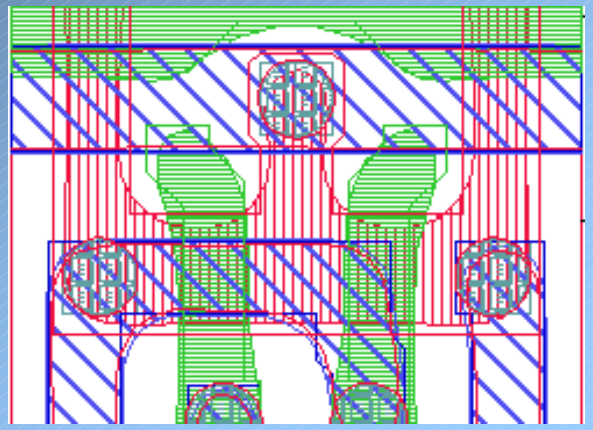

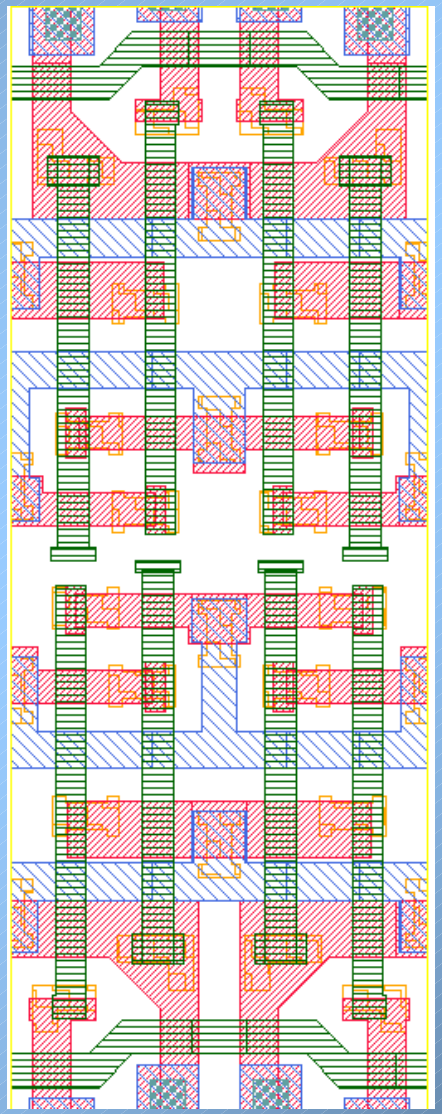

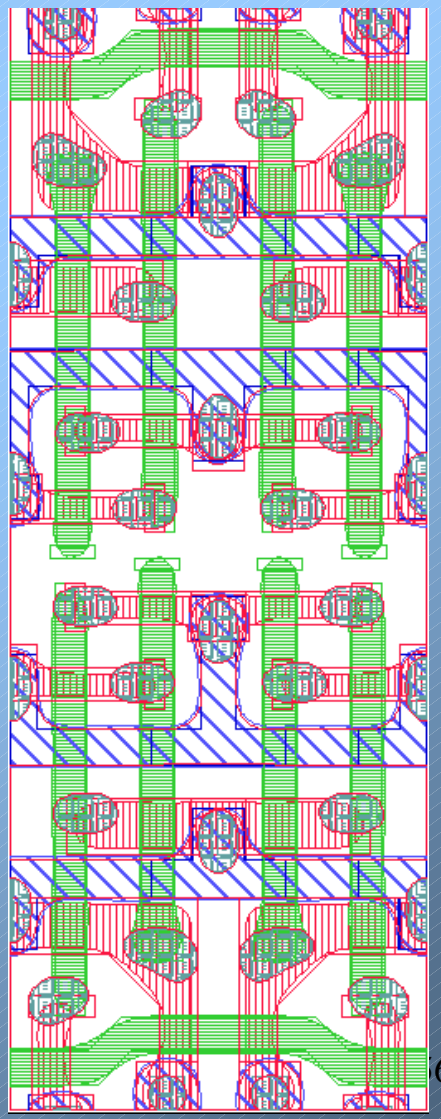

Various Related Publications in Microlithography

"Optimization Criteria for SRAM Design - Lithography Contribution," D. C. Cole, O. Bula, E. W. Conrad, D. S. Coops, W. C. Leipold, R. W. Mann, and J H. Oppold, in Optical Microlithography XII, Proc. SPIE 3679, pp. 847-859 (1999).

"Model Considerations, Calibration Issues, and Metrology Methods for Resist-Bias Model," E. W. Conrad, D. C. Cole, D. P. Paul, & E. Barouch, in Metrology, Inspection, and Process Control for Microlithography XIII, Proc. SPIE 3677, pp. 940-955 (1999).

"Using Advanced Simulation to Aid Microlithography Development," by D. C. Cole, E. Barouch, E. W. Conrad, M. Yeung. IEEE Proceedings, Vol. 89 (8), pp. 1194-1213 (2001).

"Evolution and Integration of Optimal IC Design: Performance and Manufacturing Issues," D. C. Cole, S.-Y. Baek, and X. Zhang, in Design and Process Integration for Microelectronic Manufacturing, ed. by A. Starikov, Proc. SPIE 4692B (2002).

Earlier publications describe derivation of aerial image calculation.

Casimir Force Analysis and Simulation

- Casimir-like forces involve the correlated motion of charge in nearby structures
- Originally this was purely a theoretical conjecture by Casimir in 1948, and later turned out to be a key test of quantum electrodynamics
- Now, MEMS, micro, and nano devices are finding applications of Casimir-like and van der Waals forces:
  - Atomic force microscope, both for measuring and for manipulating atoms
  - Cavity devices
  - Biological / semiconductor devices
  - Stiction in MEMS structures

Analysis for arbitrary cavity shape, with interior objects (wires, screws, …)

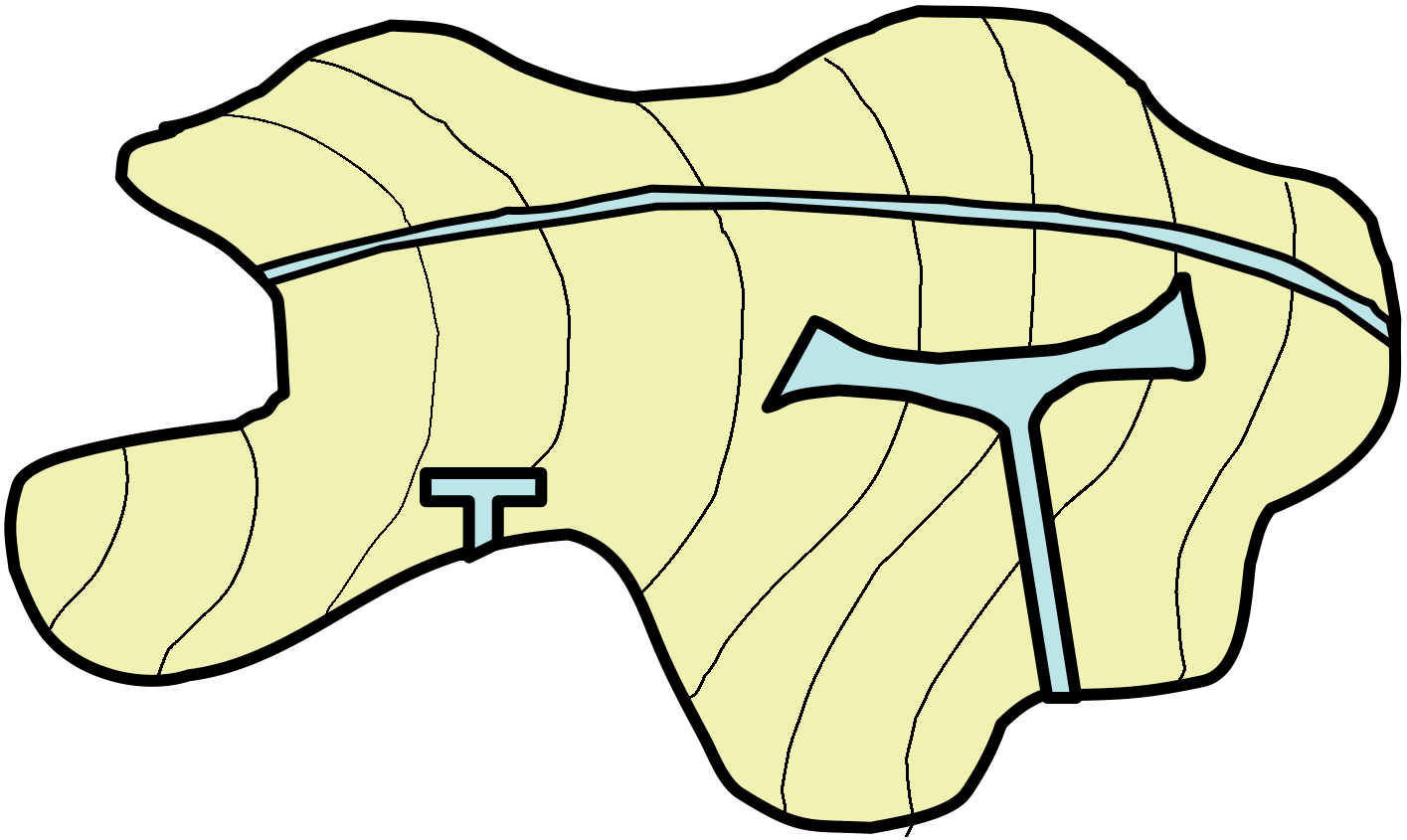

Analysis for arbitrary cavity shape, with interior objects (wires, screws, …)

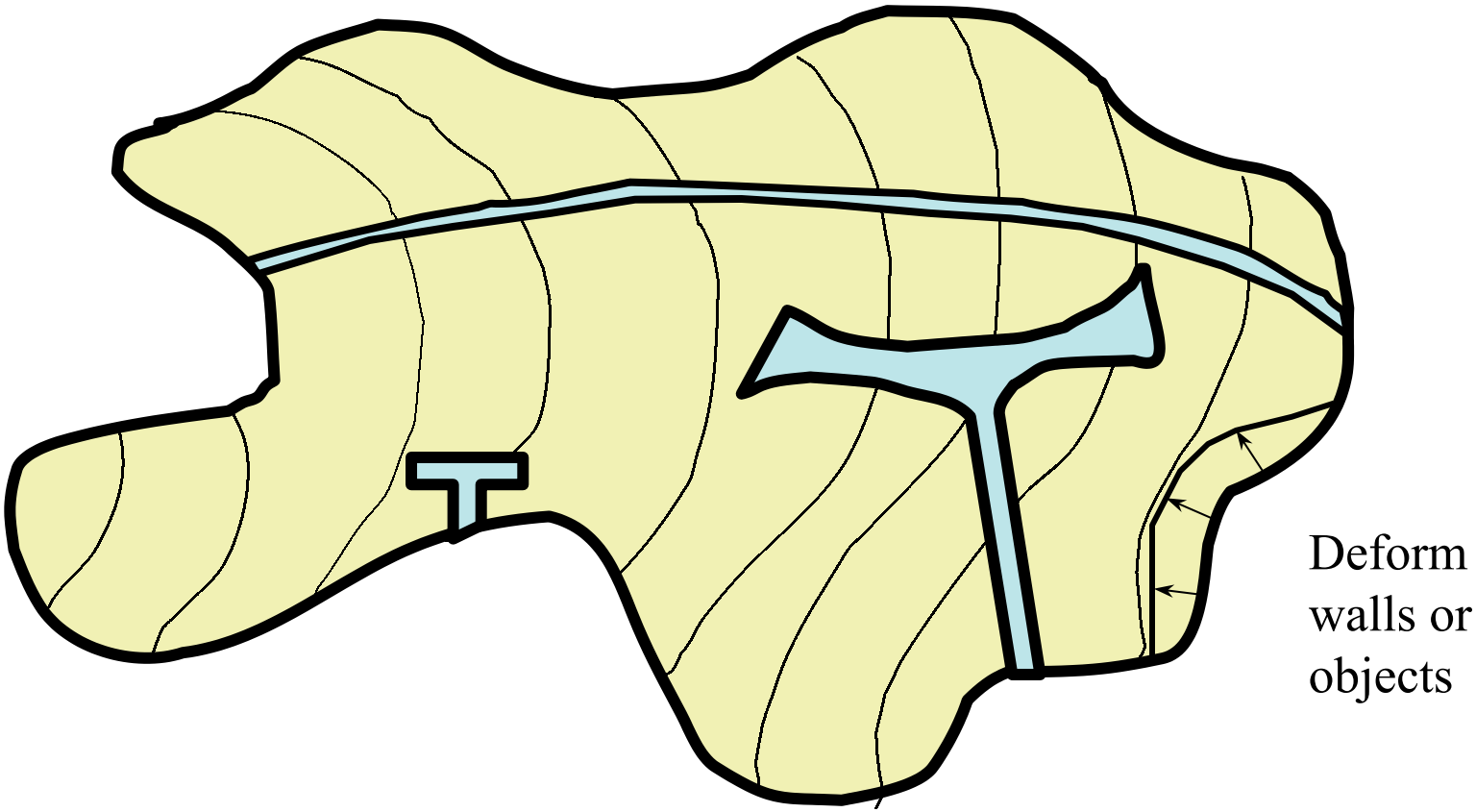

Electromagnetic cavity modes

$$\mathbf{A}(\mathbf{x},t)=\sum_{\alpha}\left[\bar{\mathbf{A}}_{\alpha}(\mathbf{x},\omega_{\alpha})e^{-i\omega_{\alpha}t}+\bar{\mathbf{A}}_{\alpha}^{*}(\mathbf{x},\omega_{\alpha})e^{i\omega_{\alpha}t}\right]$$

$$\nabla^{2}\bar{\mathbf{A}}_{\alpha}+k_{\alpha}^{2}\bar{\mathbf{A}}_{\alpha}=0\ ,\quad \nabla\cdot\bar{\mathbf{A}}_{\alpha}=0\ .$$

$$\bar{\mathbf{A}}_{\alpha}(\mathbf{x},\omega_{\alpha})=b_{\alpha}G_{\alpha}(\mathbf{x},\omega_{\alpha})\ ,\ \int_{V}d^{3}x\mathbf{G}_{\alpha}^{*}\cdot\mathbf{G}_{\beta}^{*}=\delta_{\alpha\beta}$$

Electromagnetic fields in cavity

$$\mathbf{E}_\perp(\mathbf{x},t) = i\sum_\alpha \frac{\omega_\alpha}{c}\left[\mathbf{G}_\alpha(\mathbf{x},\omega_\alpha)b_\alpha e^{-i\omega_\alpha t} - \mathbf{G}_\alpha^*(\mathbf{x},\omega_\alpha)b_\alpha^* e^{i\omega_\alpha t}\right]$$

$$\mathbf{B}(\mathbf{x},t) = \sum_\alpha\left[\nabla\times\mathbf{G}_\alpha(\mathbf{x},\omega_\alpha)b_\alpha e^{-i\omega_\alpha t} + \nabla\times\mathbf{G}_\alpha^*(\mathbf{x},\omega_\alpha)b_\alpha^* e^{i\omega_\alpha t}\right]$$

$$U = \frac{1}{8\pi}\int_V d^3x\left(\mathbf{E}_\perp^2 + \mathbf{B}^2\right) = \sum_\alpha \frac{\omega_\alpha^2 |b_\alpha|^2}{2\pi c^2}$$

$$\langle b_\alpha b_\beta\rangle = \langle b_\alpha^* b_\beta^*\rangle = 0 \qquad \langle b_\alpha b_\beta^*\rangle = p(\omega_\alpha,T)\delta_{\alpha\beta}$$

Change in internal energy

$$\delta\langle U\rangle = \frac{1}{2\pi c^2}\sum_\alpha\left[\left(\omega_\alpha\left\langle|b_\alpha|^2\right\rangle\right)\delta\omega_\alpha + \omega_\alpha\delta\left(\omega_\alpha\left\langle|b_\alpha|^2\right\rangle\right)\right]$$

$$= \frac{1}{2\pi c^2}\sum_\alpha\left\{\left[\omega_\alpha p(\omega_\alpha,T)\right]\delta\omega_\alpha + \omega_\alpha\delta\left[\omega_\alpha p(\omega_\alpha,T)\right]\right\}$$

$$\delta\omega_\alpha = \frac{\omega_\alpha}{2}\int_{\delta V} d^3x\left(|\mathbf{H}_\alpha|^2 - |\mathbf{E}_\alpha|^2\right)$$

$$\mathbf{E}_\alpha = \mathbf{G}_\alpha(\mathbf{x},\omega_\alpha)\ , \quad \mathbf{H}_\alpha = \frac{1}{k_\alpha}\nabla\times\mathbf{G}_\alpha(\mathbf{x},\omega_\alpha)\ .$$

Lorentz force

$$\int_V d^3x \left[\rho(\mathbf{x},t)\mathbf{E}(\mathbf{x},t) + \frac{1}{c}\mathbf{J}(\mathbf{x},t)\times\mathbf{B}(\mathbf{x},t) \right]_i$$

$$= \oint_S d^2x \sum_{j=1}^{3} n_j T_{ij}(\mathbf{x},t) - \frac{1}{c^2}\frac{d}{dt}\int_V d^3x S_i(\mathbf{x},t) \quad ,$$

where: $T_{ij} = \frac{1}{4\pi}\left[E_i E_j + B_i B_j - \delta_{ij}\frac{1}{2}(\mathbf{E}\cdot\mathbf{E} + \mathbf{B}\cdot\mathbf{B}) \right]$

$$\mathbf{S}(\mathbf{x},t) = \frac{c}{4\pi}(\mathbf{E}\times\mathbf{B})$$

Work done in deformation of small surface element

$$\int_{\delta V} d^3x \left\langle \rho(\mathbf{x},t)\mathbf{E}(\mathbf{x},t) + \frac{1}{c}\mathbf{J}(\mathbf{x},t)\times\mathbf{B}(\mathbf{x},t) \right\rangle_i = \oint_{\delta S} d^2x \sum_{j=1}^{3} n_j \left\langle T_{ij}(\mathbf{x},t) \right\rangle$$

$$dA\left\langle \mathbf{F}_{\text{external}} \right\rangle \cdot \delta\mathbf{z} = -dA\int_{\delta V} d^3x \left\langle \rho\mathbf{E} + \frac{1}{c}\mathbf{J}\times\mathbf{B} \right\rangle \cdot \delta\mathbf{z}(\mathbf{x})$$

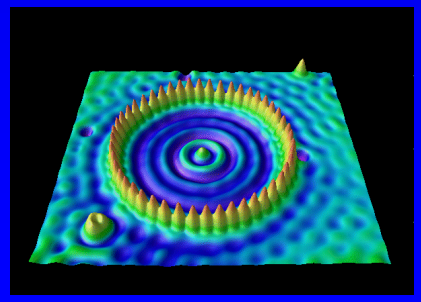

Work done during deformation:

$$\langle W \rangle = -\int_S d^2x \sum_{i,j=1}^{3} (\hat{\mathbf{n}})_j \langle T_{ij} \rangle \delta \mathbf{z}_i(\mathbf{x})$$

$$= -\frac{1}{4\pi}\int_S d^2x \left\langle (\hat{\mathbf{n}}\cdot\mathbf{E})\mathbf{E} + (\hat{\mathbf{n}}\cdot\mathbf{B})\mathbf{B} - \frac{1}{2}\left(E^2 + B^2\right)\hat{\mathbf{n}} \right\rangle \cdot \delta\mathbf{z}$$

$$= -\frac{1}{4\pi}\int_S d^2x (\hat{\mathbf{n}}\cdot\delta\mathbf{z})\frac{1}{2}\langle E^2 - B^2 \rangle = -\frac{1}{8\pi}\int_{\delta V} d^3x \langle E^2 - B^2 \rangle$$

$$= -\frac{1}{2\pi}\sum_\alpha \langle |b_\alpha|^2 \rangle \frac{1}{2}\int_{\delta V} d^3x \left[\left(\frac{\omega_\alpha}{c}\right)^2 |\mathbf{E}_\alpha|^2 - |k_\alpha \mathbf{H}_\alpha|^2 \right]$$

$$= +\frac{1}{2\pi c^2}\sum_\alpha \left(\langle |b_\alpha|^2 \rangle \omega_\alpha \right) \delta(\omega_\alpha)$$

First law of thermodynamics

$$\langle Q \rangle = \Delta \langle U_{\text{internal}} \rangle - \langle W \rangle$$

$$= \frac{1}{2\pi c^2} \sum_{\alpha} \left[\left(\omega_\alpha \left\langle |b_\alpha|^2 \right\rangle \right) \delta\omega_\alpha + \omega_\alpha \delta \left(\omega_\alpha \left\langle |b_\alpha|^2 \right\rangle \right) \right]$$

$$- \frac{1}{2\pi c^2} \sum_{\alpha} \left(\left\langle |b_\alpha|^2 \right\rangle \omega_\alpha \right) \delta(\omega_\alpha)$$

$$= \frac{1}{2\pi c^2} \sum_{\alpha} \omega_\alpha \delta(\omega_\alpha p(\omega_\alpha, T))$$

Future work

- Should be possible to extend work to arbitrarily shaped cavities of general dielectric materials, with charged regions.
- The possibility now opens to write simulation programs that combine more conventional semiconductor simulation methods with Casimir interactions for MEMS like devices.
- More than one cavity, and separate modes, form basis for testing thermodynamic ideas.
- Reversible processes form basis for analyzing irreversible and steady-state processes

References

- Cole, D. C., "Thermodynamics of Blackbody Radiation via Classical Physics for Arbitrarily Shaped Cavities with Perfectly Conducting Walls," Found. Physics 30, Nov. 2000.
- Cole, D. C., "Cross-term Conservation Relationships for Electromagnetic Energy, Linear Momentum, and Angular Momentum," Found. Physics 29, 1999.
- Cole, D. C., "Reinvestigation of the Thermodynamics of Blackbody Radiation via Classical Physics," Phys. Rev. A 45, 8471-8489 (1992).
- Cole, D. C., "Entropy and Other Thermodynamic Properties of Classical Electromagnetic Thermal Radiation," Phys. Rev. A 42, 7006-7024 (1990).
- Cole, D. C., "Derivation of the Classical Electromagnetic Zero-Point Radiation Spectrum via a Classical Thermodynamic Operation Involving van der Waals Forces," Phys. Rev. A 42, 1847-1862 (1990).
- Kupiszewska, D., "Casimir Effect in Absorbing Media," Phys. Rev. A 46, 2286-2294 (1992).

(Backup slide)

Thermodynamic Analysis Explored

- Early blackbody thermodynamic analysis contained innocuous & physically appealing assumptions, resulting in significant differences from nature.
- Effects due to Casimir-like forces and van der Waals forces could not be taken into account.
- Stéfan-Boltzmann & Wien analysis contained flaw.
- Ultraviolet catastrophe, third law analysis for radiation, specific heats, & other effects & properties, significantly hindered in early analysis, largely by not taking into account the possibility of ZP radiation & appropriately subtracting and taking differences.

(Backup slide)

Obtain derivation for ZP form (T=0)

Thus, to have $\langle Q \rangle = 0$ for all reversible deformations (definition of $T = 0$), then

$$p(\omega, T = 0) = \frac{K}{\omega}$$

This enables a derivation of the functional form for the electromagnetic zero-point energy of ($K = \pi c^2 \hbar$)

$$\langle U_{T=0} \rangle = \sum_{\alpha} \frac{\hbar \omega_{\alpha}}{2} \quad .$$

(Backup slide)

Different means of calculating at T=0

Moreover, we see that calculations at $T = 0$ can now be carried out via a change in internal energy type calculation of

$$0 = \langle Q \rangle = \Delta \langle U_{\text{internal}} \rangle - \langle W \rangle$$

$$\Delta \langle U_{\text{internal}} \rangle \underset{T=0}{=} \Delta \left(\sum_{\alpha} \frac{\hbar \omega_{\alpha}}{2} \right)_{\text{inside}} + \Delta \left(\sum_{\alpha} \frac{\hbar \omega_{\alpha}}{2} \right)_{\text{outside}}$$

which equals work done during quasistatic displacement

$$\langle W \rangle = \int_S d^2x \langle \mathbf{F}_{\text{external}} \rangle \cdot \delta \mathbf{z} = -\int_S d^2x \sum_{i,j=1}^{3} (\hat{\mathbf{n}})_j \langle T_{ij} \rangle \delta \mathbf{z}_i (\mathbf{x}) \ .$$

Simulation of Physical Processes (Backup slide)

MOSFET Printed Using Positive Resist

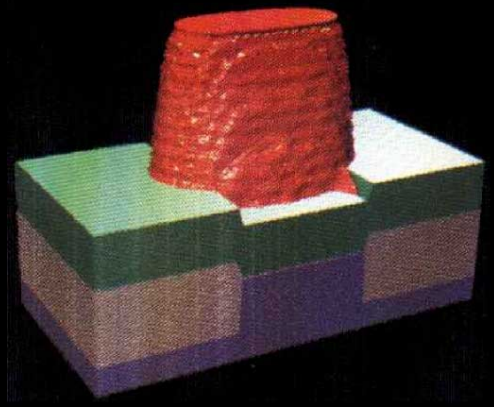

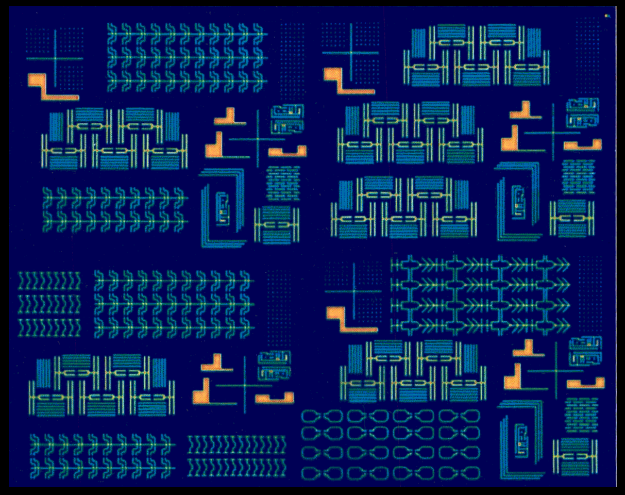

Contact Hole Printed
Using Negative Resist

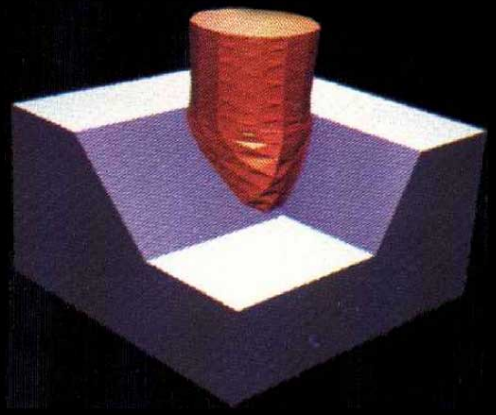

Simulation of Physical Processes (Backup slide)